Macromolecules

pubs.acs.org/Macromolecules

Perspective

Polymer Adhesion: Seeking New Solutions for an Old Problem[#]

Guido Raos* and Bruno Zappone*

Cite This: *Macromolecules* 2021, 54, 10617−10644

Read Online

ACCESS | Metrics & More | Article Recommendations

ABSTRACT: Polymer adhesion is ubiquitous in both the natural world and human technology. It is also a complex multiscale phenomenon, such that the solution of adhesion problems requires a convergence of chemistry, physics, and engineering. In this Perspective, we provide an overview of some of the fundamental concepts that have emerged in the field of polymer adhesion, discuss recent work, and identify challenges in three specific areas: (a) theories and simulations, with an emphasis on problems involving chain scission; (b) experimental methods for measuring forces and characterizing interfaces at the molecular scale; and (c) strategies inspired by living organisms to generate underwater adhesion.

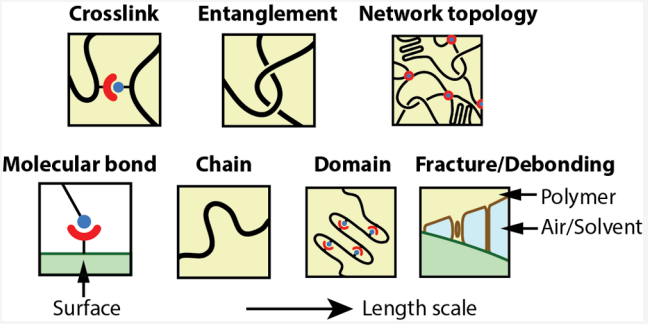

INTRODUCTION

Polymeric materials derived from tree resin (pitch and tar), animal skin and bones, and natural rubber have been used as adhesives for millennia, long before Staudinger recognized polymer molecules as chainlike sequences of covalently bonded units.[1] The most abundant polymeric biomolecule in animal connective tissues, collagen protein, was named in reference to its ability to produce a glue, or *κόλλα* in ancient Greek and *colla* in modern Italian. The term "colloid" originally referred to all types of ill-defined and sticky forms of matter—including polymers—which could not be purified by crystallization. The English word glue derives from the Latin *glutinum*, which is also related to gluten—another sticky proteinaceous material extracted from plants.

Today, synthetic polymers can be engineered to have high mechanical strength or deformability, electrical and thermal conductivity, optical transparency, chemical resistance, and biocompatibility to satisfy a growing demand for adhesives, sealants, and coatings in advanced and emerging technologies such as microelectronics, 3D-printing, regenerative medicine, and tissue engineering.[2] Polymer adhesives are also replacing traditional joining methods such as soldering, bolting, and screwing, particularly in aerospace and automotive engineering, because they are lighter, generate little stress concentrations, and are more resistant to fatigue.[3] This versatility stems from the variety of molecular parameters that define a polymer, including the physicochemical properties of the main chain and side groups, molecular weight, degree of polymerization, block architecture, topology, and solid-state morphology.

Adhesion between two materials requires strong interactions across their interface, with a nonvanishing contact area. In polymers, as in other materials, adhesion can be promoted by introducing chemical groups that enable strong interfacial interactions. Unlike other materials, however, polymers can be engineered to express a wide spectrum of bulk viscoelastic properties. In particular, they can be applied to surfaces as fluids (before polymerization, cross-linking or resolidification) or soft viscoelastic materials, so as to comply and conform to the surfaces, and maximize the adhesive contact area. In contrast, rigid materials such as metals, ceramics, or glass come into contact with their hard asperities, creating a sparse interface with a small contact area and weak adhesion. The flexible design of viscoelastic properties also allows controlling the distribution, storage, and dissipation of energy within a deformed polymer material, reducing adhesive and cohesive failures. After a century of polymer science, and thanks also to the work of Giuseppe Allegra (see Figure 1, as well as a few references spread throughout this Perspective), the linear viscoelastic properties of polymers and their elastic strength (i.e., resistance to non-reversible plastic deformations) are fairly well-understood, starting from fundamental statistical mechanical principles.[4−8] On the other hand, their interfacial properties and nonlinear viscoelastic response are still the focus of intense research efforts, with important implications for adhesion technology. Polymer materials can show a high toughness, i.e., the ability to sustain large and irreversible mechanical deformations by absorbing large amounts of energy without breaking completely, and may

Received: May 31, 2021
Revised: November 4, 2021
Published: November 28, 2021

https://doi.org/10.1021/acs.macromol.1c01182
Macromolecules 2021, 54, 10617−10644

Figure 1. Giuseppe Allegra in 1996.

even heal after the stress is released. Figure 2 anticipates graphically some key features and mechanisms that are responsible for these properties and will be extensively discussed in the following.

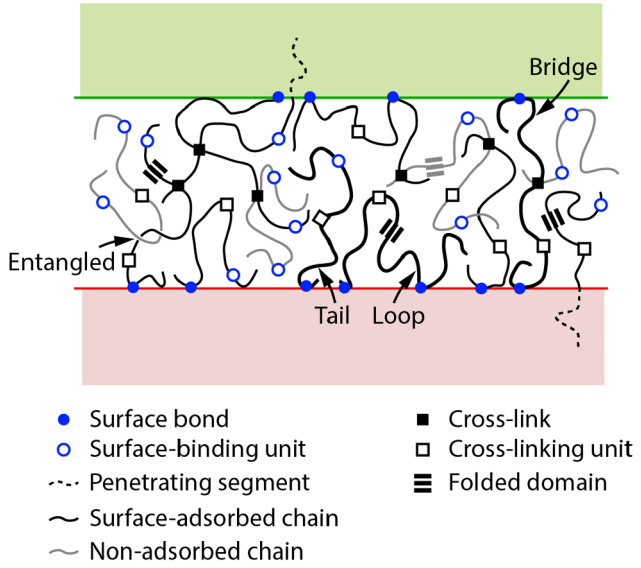

Figure 2. Schematic illustration of the internal structure of an adhesive polymer film between two solid surfaces, showing molecular features relevant to surface force generation.

Virtually all modern adhesives are based on polymers, and all aspects of polymer chemistry and physics may in principle be relevant for controlling adhesion phenomena. An application-based classification of adhesives may give us an idea of the vastness of the subject.[2,3] *Structural* adhesives are used to bind high-strength materials such as metals and composites. They typically are highly cross-linked thermosetting polymers and can be based on a range of chemistries, such as epoxides and cyanoacrylates. Structural adhesives include the earliest synthetic polymer (Bakelite), but they are also employed in high-tech sectors such as aerospace and electronics. *Elastomer-based* adhesives include pressure-sensitive adhesives, which are used in all types of sticky tape, and rubber-based adhesives that may have some structural role (e.g., in furniture and construction) and are usually formulated as a mixture with an organic solvent or water, which evaporates after application. *Thermoplastic* adhesives include hot-melt adhesives that are applied in the melt state and gain strength upon resolidification or crystallization (e.g., in book binding) and polyvinyl acetate-based emulsions (e.g., the "white glue" used in every household). The natural polymers mentioned above may also be included in this class. One important emerging category, not included in this traditional classification, is that of hydrogel adhesives increasingly used in the biomedical field.[9−13]

Because of the vastness of the topic, we will not attempt to cover every aspect of polymer adhesion. Rather, our aim is to highlight some general physicochemical principles and point to a few emerging topics. An important question that motivated this Perspective is how to predict the adhesive and mechanical properties of a polymer material starting from the microscopic description of a dynamical network of coiled, interwoven, and cross-linked polymer chains (Figure 2). It is striking that, even though polymers have been adopted because of their unique mechanical properties, today it is probably easier to compute from first-principles their optical or electrical properties than their elastic modulus or toughness. This is a fascinating question with enormous practical implications in surface and adhesion technology.

One key concept underlying this Perspective is that polymer adhesion is a complex, multiscale phenomenon. For example, a hydrogen bond donor and an acceptor must come within 0.5 nm from each other with a specific orientation in order to establish interaction, but many such interactions must act cooperatively over much larger length scales (at least hundreds of nanometers) in order to be effective. Any discussion of adhesion should encompass these scales and phenomena, bridging the molecular and the continuum description of materials. This is challenging also for the authors of this Perspective, because the intended readers may come from different backgrounds (chemistry, physics, biology, or engineering disciplines), lack some essential pieces of the puzzle, or use the same terms to indicate different things. In order to face this challenge, in addition to indicating some current and future research topics, we have chosen to provide some of the essential definitions and basic concepts. We hope that, by making this Perspective reasonably self-contained, we will have done a reasonable service to the community of researchers, especially to the newcomers to the field. Following the fundamentals, we focus on some of the emerging areas and current challenges. These include theories and simulations of adhesives and adhesion phenomena, experimental methods for characterizing polymer interfaces and directly measuring adhesive forces at the nanoscale, and strategies for generating adhesion on wet surfaces and in aqueous environments.

FUNDAMENTALS

Stripped down to its essence, adhesion is about the mechanical behavior of the interface between two materials or of one material (the adhesive) joining the surfaces of two other materials (the adherends). Throughout this Perspective, we assume that the adhesive is a polymer, whereas the substrate or adherends may be any material (metals, ceramics, glasses, other polymers, biological tissues, etc.). Let us then start by giving a few essential definitions and concepts related to material interfaces and mechanics.[2,14] These mostly involve macroscopic properties and could be given without making reference to the (macro)molecular nature of the materials or to a specific experimental setup. Nonetheless we shall occasionally make such references, in order to clarify these concepts through examples.

https://doi.org/10.1021/acs.macromol.1c01182
Macromolecules 2021, 54, 10617−10644

Interfacial Energies and Wetting. The molecules at the surface of a solid or liquid experience different interactions from those in the bulk. When the interface is "atomically sharp", as is the case for fluids well below their critical temperature or the cleavage plane of a layered crystalline solid such as mica, graphite, and molybdenite, the thickness of this interface can be identified with the characteristic range of intermolecular forces.[15] This is of the order of 1 nm, including the ubiquitous dispersion forces, short-range specific interactions such as hydrogen bonding, and also electrostatic interactions in ionic solutions at physiological concentrations (due to Debye–Hückel screening of charge–charge interactions). Following Gibbs, when this thickness is much smaller than any other relevant length scale in the system, the "interface" can be described as an ideal two-dimensional diving surface.[16] Notice that the size of macromolecules can greatly exceed the range of intermolecular forces. For example, the radius of gyration of an unperturbed polystyrene chain with molecular weight $M_W = 3 \times 10^5$ g/mol is of the order of 15 nm.[17] All the macromolecules whose centers-of-mass are within that distance from the nominal interface will be significantly perturbed by it.[18] In this case, it is common to speak of an "interphase" of finite thickness, with structural and dynamical properties distinct from those of the bulk, especially in the neighborhood of the polymer's glass transition temperature.[19,20]

The surface (free) energy (γ_i) of a material collects the contributions to its free energy that are proportional to the interfacial area (unlike the ordinary "bulk" contributions that are proportional to its volume or mass). Formally, it can be defined as

$$\gamma_i = \left.\frac{\partial F_i}{\partial A}\right|_{n,V,T} = \left.\frac{\partial G_i}{\partial A}\right|_{n,P,T} \tag{1}$$

where F_i and G_i are the Helmhotz and Gibbs free energies of phase i; A is the interfacial area; n is the number of molecules (of each species, in a mixture); and V, P, and T are the volume, pressure, and absolute temperature, respectively. The surface energy is a thermodynamically well-defined equilibrium property for both solids and liquids. In the latter case, it is also known as "surface tension", because it measures a force per unit length that opposes surface deformations, as if the surface were a thin elastic membrane. One value worth remembering, because of its connection with everyday experience, is the surface tension of water at room temperature, $\gamma_w = 73$ mN/m. The surface tension of liquid polyethylene (PE) is about $\gamma_{PE} = 27$ mN/m for high-M_w polyethylene chains at 150 °C, and decreases as M_n^{-1} on decreasing the chain length due to the effect of the chain terminals.[21] Poly(tetrafluoroethylene) (PTFE), a prototypical low surface energy polymer, has $\gamma_{PTFE} = 18$ mN/m around the same temperature.

Let us consider the separation of a block of material i in vacuum or in air, by *reversibly* cutting through it. Note that the requirement of thermodynamic reversibility is not easily achieved in the case of polymers; we shall return to elaborate on this point later. The *work of cohesion* spent to perform this operation is

$$W_{ii} = 2\gamma_i \tag{2}$$

where the factor 2 derives from the fact that two identical surfaces are created on opposite sides of the cut. This quantity enters Griffith's criterion for the propagation of a crack within a brittle material (i.e., a material without any energy dissipation mechanisms) as the minimum value for the strain energy release rate—the decrease in stored elastic energy per unit area of the new interface.[22] If the new surfaces are created by cutting between two unlike materials, the analogous quantity is the *work of adhesion* given by the Dupré equation:

$$W_{ij} = \gamma_i + \gamma_j - \gamma_{ij} \tag{3}$$

where γ_{ij} is the energy associated with the interface between i and j.

As a rule of thumb, the work of cohesion is in the 10–100 mN/m range for noncovalent interactions and increases by at least 1 order of magnitude when surface separation involves the rupture of covalent bonds. These estimates can be justified by taking the ratio between the interaction or bond energies occurring across an area and the area itself. Works of adhesion are generally smaller and more variable depending on the materials, as they result from the subtraction of different, often comparable contributions (see again eq 3). Nonetheless they are always positive, reflecting the fact that two condensed materials prefer to stay in contact rather than being exposed to vacuum (or air).

Water-insoluble materials are classified as hydrophilic, hydrophobic, or neutral according to how a small water droplet behaves after being placed on the material's surface in air.[15] The behavior depends on the work of adhesion between the surface (i) and water (w), W_{iw}, compared to the surface tension of water, γ_w. Namely, when $0 < W_{iw} < 2\gamma_w$, water forms a droplet with spherical cap shape and contact angle θ given by the Young–Dupré equation:

$$\cos\theta = \frac{W_{iw}}{\gamma_w} - 1 \tag{4}$$

When $W_{iw} \geq 2\gamma_w$, the droplet is unstable and spreads into a continuous wetting film. When $W_{iw} = 0$, water completely retracts from the surface into a spherical droplet or "de-wets". Conventionally, the surface is considered hydrophilic if $\theta < 30°$ or wetting occurs, hydrophobic if $\theta > 70°$ or dewetting occurs, and neutral otherwise.

Elasticity of Polymers. As mentioned above, in addition to its *surface* free energies, the *bulk* mechanical or viscoelastic properties of a material are crucial for its adhesive behavior. For an isotropic material, restricting ourselves to the domain of linear elasticity (i.e., in the limit of small and slow deformations), these are fully characterized by two independent material parameters. Usually, these are taken to be the bulk modulus (K) and the shear modulus (G), or the Young modulus (E) and the Poisson ratio (ν). The first three have dimensions of pressure or energy per unit volume and therefore are measured in Pa (= 1 N/m^2 = 1 J/m^3), while the latter is adimensional. They are related as follows:[23]

$$E = \frac{9KG}{3K+G} \quad \text{and} \quad \nu = \frac{3K-2G}{2(3K+G)}$$
$$K = \frac{E}{3(1-2\nu)} \quad \text{and} \quad G = \frac{E}{2(1+\nu)} \tag{5}$$

These elastic moduli relate the stress (σ_{pq}) to the strain (ϵ_{rs}), where the subscripts indicate that these are tensor quantities. For the purpose of illustration, let us consider the simple case of a material being stretched or compressed uniformly along one direction (say z) and allowed to relax along the orthogonal

https://doi.org/10.1021/acs.macromol.1c01182
Macromolecules 2021, 54, 10617–10644

directions (x and y). The off-diagonal strain components are then zero, whereas the diagonal ones are given by

$$\epsilon_{zz} = \frac{d - d_0}{d_0} \quad \epsilon_{xx} = \epsilon_{yy} = -\nu\epsilon_{zz} \tag{6}$$

where d and d_0 denote the deformed and undeformed sample length, respectively. The resulting stress is

$$\sigma_{zz} = E\epsilon_{zz} \quad \sigma_{xx} = \sigma_{yy} = 0 \tag{7}$$

However, if we consider a thin layer of adhesive material bonded to two rigid surfaces being pulled away from each other, the lateral dimensions of the sample will not be able to relax. In this case one has

$$\epsilon_{zz} = \frac{d - d_0}{d_0} \quad \epsilon_{xx} = \epsilon_{yy} = 0 \tag{8}$$

and[23]

$$\sigma_{zz} = \frac{E(1-\nu)}{(1+\nu)(1-2\nu)}\epsilon_{zz}$$
$$\sigma_{xx} = \sigma_{yy} = \frac{E\nu}{(1+\nu)(1-2\nu)}\epsilon_{zz} \tag{9}$$

For many soft solids such as rubbers and pressure-sensitive adhesives, $K \gg G$ and ν approaches its limit value of 0.5 from below. This means that the material tends to deform without volume changes, unless it is constrained in some way (see above). Note that the stress calculated from eq 9 is much larger than that obtained from eq 7, when $\nu > 0.45$.

Typical values for E are 1−10 kPa for gels, 1−10 MPa for rubber, 1 GPa for plastics, and 100 GPa for hard materials such as metals and ceramics. This range of elastic moduli can also be found in living tissues, with brain and bones at the two extremes of the scale.[24] Thus, while surface free energies are restricted within 2 or 3 orders of magnitude, the mechanical properties of the contacting materials can differ by more than 8 orders of magnitude. This observation explains why mechanics may overtake intermolecular interactions when it comes to interpreting and controlling adhesion phenomena. Note that controlling the elastic modulus can also be exploited to suppress unwanted adhesion phenomena. For example, the built-in nanoscale heterogeneity in the elastic properties of soft nanocomposites has been exploited to develop durable ice-phobic coatings,[25] following a model for interfacial mechanical instabilities by Chaudhury and Kim.[26]

Curved Contact Geometries and the JKR Model. The relative importance of adhesive and mechanical forces depends on the length scale.[27,28] The ratio of the work of adhesion between two materials and their Young modulus (W_{ij} and E_i or E_j, respectively, measured in J/m^2 and J/m^3) defines a characteristic length scale known as the *elasto-adhesive length* l_i.[29] If one material is much softer than the other ($E_i \ll E_j$), it will bear the whole deformation, and we may simply write

$$l_i = \frac{W_{ij}}{E_i} \tag{10}$$

Figure 3a illustrates how interfacial forces dominate at length scales smaller than l_i (e.g., a material may undergo large deformations in order to optimize these interactions), but the opposite occurs at larger length scales. Taking as an example the relatively large value W_{ij} = 0.1 N/m^2 and using the previously quoted values for the elastic moduli, we find l_i = 0.1 mm (gel on steel), 0.1 μm (rubber on steel), or <1 nm (plastic on steel).

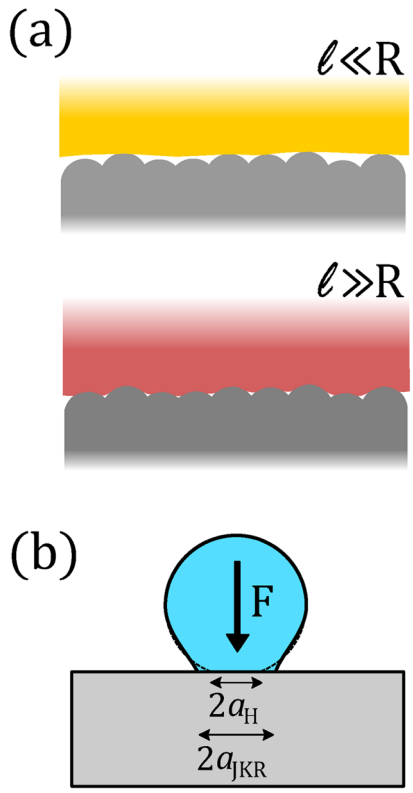

Figure 3. Coupling between interfacial energy and elastic deformation. (a) Adhesion between a rigid substrate with characteristic length scale R (radius of the protrusions) and an adhesive with small or large elasto-adhesive length scale l. (b) Scheme of the Johnson−Kendall−Roberts experiment, comparing the Hertz and JKR radii for a given applied force F.

The coupling between mechanical deformation and adhesion can be described at the macroscopic scale using the JKR model, named after Johnson, Kendall, and Roberts.[30,31] Their seminal work, which turned 50 this year, has been extremely useful to experimentalists and spurred several theoretical studies.[32] The JKR model describes the behavior of two elastic spheres pressed against each other under a mechanical force F. The work of adhesion between the materials making up the spheres is W_{12}. The model generalizes a previous one by Hertz, who considered the case of mechanical contact without adhesion (i.e., for W_{12} = 0).[23] The main result of the JKR model is a closed analytical expression for the radius a of the contact region between the spheres. For simplicity, we give it here for the special case of an elastic sphere (radius R, Young modulus E, and Poisson ratio ν) pressed against a perfectly flat and rigid substrate (see Figure 3b). The expression for the contact radius can be derived from the more general solution[30] by taking the limit when the radius of one sphere and the corresponding modulus both go to infinity, and it is

$$a^3 = \frac{3(1-\nu^2)}{4E}R\left[F + 3\pi W_{12}R + \sqrt{6\pi W_{12}RF + (3\pi W_{12}R)^2}\right] \tag{11}$$

Equation 11 can be used to fit the measured contact radii a as a function of the applied force F, thus providing the value of the

https://doi.org/10.1021/acs.macromol.1c01182
Macromolecules 2021, 54, 10617−10644

work of adhesion W_{12} (or the surface free energy of solids, when the two contacting materials are identical). Note that, for a given applied force, the radius calculated from the JKR equation is always larger than the one obtained in the absence of adhesive forces (Hertz limit). Equation 11 can be rearranged to give the contact radius at zero applied force:

$$\frac{a_0}{R} = \left[\frac{9}{2}\pi\frac{(1-\nu^2)}{E}\frac{W_{12}}{R}\right]^{1/3} \sim \left(\frac{l}{R}\right)^{1/3} \quad (F=0) \tag{12}$$

showing that the combined effect of surface forces and elasticity does indeed depend on the relative values of the l length scale (eq 10) and the object size R. Note also that eq 11 admits solutions also for negative values of the force, for $F \geq -\frac{3}{2}\pi W_{12}R$. This limit value, known as *adhesion* or *pull-off* force, is independent of the elastic constants E and ν but depends on the radius R and is usually presented as F/R to allow comparison between different surface geometries. The application of the JKR experiment to polymers, especially for elastomer adhesion problems, was pioneered by Chaudhury[33] and quickly adopted by several other authors.[34−36] An early overview of its strengths and challenges (e.g., application to systems displaying hysteresis and viscoelastic phenomena) was given by Tirrell.[37]

The Importance of Nonequilibrium Processes. So far, we have assumed that the systems are at equilibrium and all processes preserve thermodynamic reversibility at all times. For example, in an experimental test of the JKR model, surface attachment and detachment should occur so slowly that the forces and radii measured during attachment and detachment are identical. However, this is not usually the case, especially when the elastic sphere is very soft and "sticky" on the substrate. Similarly, contact angle measurements often depend on the previous "history" of the sessile drop. In particular, it is often necessary to distinguish between an advancing and a receding contact angle, and these may differ by up to tens of degrees.[14,15] All this points to the importance of irreversibility, hysteresis, and energy dissipation. Far from being a nuisance, these phenomena are in fact essential and can be exploited in order to ensure good adhesion in a variety of practical situations.[2,29]

The *practical work of adhesion* measures the toughness of the adhesive bond. It is obtained from the integral of the stress−strain or force−displacement curve in a JKR-like experiment or tack test during surface retraction. In the latter case, assuming that the experiments consist of detaching materials i and j, it is simply given by

$$\Gamma_{ij}(v, \mathcal{H}) = -\int_0^{D^*} F_{ij}(D, v, \mathcal{H})\,\mathrm{d}D \tag{13}$$

where D is the surface separation distance and the integral of the force F_{ij} is extended up to the full breakup point D^*, where the force falls to zero. The minus sign depends on the fact that the force is taken to be positive when the adherends are pressed together (as in the previous discussion of the JKR experiment, see the arrow in Figure 3). The dependence of the result on the pulling velocity $v = \mathrm{d}D/\mathrm{d}t$ and on the previous "history" $\mathcal{H}$ of the system (e.g., how it has been prepared, how long have the materials been in and out of contact, and how many times) have been explicitly indicated. In principle, one should have

$$W_{ij} = \lim_{v\to 0} \Gamma_{ij}(v, \mathcal{H}) \tag{14}$$

but in practice, because of the presence of energy dissipation phenomena, one often observes

$$\Gamma_{ij}(v, \mathcal{H}) \gg W_{ij} \tag{15}$$

for all practically applicable velocities. In fact, practical works of adhesion may be as large as 10^3-10^4 N/m, comparable with the intrinsic toughness of rubber.[9,38,39] These values imply a 100- or even 1000-fold increase over the thermodynamic W_{ij}'s.

In view of the predominance of dissipation for the strength of adhesive bonds, it is important to develop some insight into its physical origins. First, one should consider the viscoelasticity of polymer materials.[40−42] Considering for example a cyclic elongational deformation at a frequency ω, the recorded stress has both an in-phase and an out-of-phase component. These can be combined within the complex viscoelastic modulus $E^*(\omega) = E'(\omega) + \mathrm{i}E''(\omega)$. The fraction of mechanical work that is dissipated as heat is given by $\tan[\delta(\omega)] = E''(\omega)/E'(\omega)$. Viscoelastic dissipation is especially important at temperatures close to the polymer's glass transition temperature, which may differ from its bulk value if the thickness of the adhesive layer is of the order of tens of nanometers.[19,20] Away from the glass transition, viscoelastic dissipation is less relevant and may almost vanish if we consider wet adhesives (see below). Other dissipation mechanisms may then take over, especially at large deformations.

Polymer Interactions and Dissipation at the Molecular Scale. Mechanical strength and toughness are often, but not always,[43] found to be mutually exclusive in a polymer material.[44] For example, increasing the strength or density of covalent bonds in a homogeneous elastomer such as poly(dimethylsiloxane) (PDMS) creates a stiffer and stronger polymer, but it also increases brittleness. Conversely, physical bonds that can break and reform, such as chain entanglement and hydrogen bonds, do not effectively increase elastic strength, but allow the polymer material to flow and remodel under a mechanical deformation, dissipating energy and slowing down fracture propagation. Thus, optimizing adhesion requires a balanced mix of different types of bonds and interactions, both at the interfaces and within the adhesive layer (see Figure 2).

Excluding the ubiquitous viscoelasticity, the most important dissipation mechanism is probably the breaking of structures formed by the association of polymer segments via chemical bonds and physical (noncovalent) interactions. These associations can be "cross-links" between different chains or noncontiguous polymer segments of the same chain or can be intrachain clusters of contiguous segments, possibly folded in a defined domain structure (Figure 2). Examples of physical associations that have been used to tune adhesion and energy dissipation in polymer materials include electrostatic (charge−charge) interactions, hydrogen bonds, clustering of hydrophilic groups (within a nonpolar matrix or solvent), hydrophobic interactions (within a polar matrix or water), metal coordination bonds, cation−π interactions, and polypeptide β-sheet domains.[45−48] Given enough time, these interactions may reform after breaking, thus restoring or "healing" the properties of the polymer adhesive. Covalent bonds may also dissipate a lot of energy, especially when they are part of a long polymer chain.[49] Energy dissipation by chain scission is exploited also for the toughening of "double" networks and gels.[50−52] Once broken, however, these chains are essentially lost as the resulting radicals—chain scission is usually homolytic—tend to undergo further degradation reactions without recombining. Transition metal coordination bonds have energies that are comparable to those of covalent bonds but can reform after breaking.[48] In the special case of polymer-on-polymer adhesion, interfacial chain

https://doi.org/10.1021/acs.macromol.1c01182
Macromolecules 2021, 54, 10617−10644

entanglements and the resulting pullout work can provide an additional, important toughening mechanism (Figure 2).[53] This is effectively exploited in the assembly of automotive tires from different rubber components[41] and in hydrogel adhesion.[12]

MODELS FOR POLYMER ADHESION

Macromolecular and Continuum Models. In principle, any theoretical or computational study of the mechanics and interfacial properties of polymers might be relevant for adhesion problems. Possible approaches include electronic structure calculations, statistical mechanical theories, molecular and mesoscale simulations, continuum mechanics, as well as multiscale combinations of these methods. In order to circumscribe the subject, we shall focus on models that attempt to predict or describe the mechanical properties of polymer adhesives, neglecting numerous studies of structural or dynamical properties of adsorbed polymer layers, confined films and interphases under equilibrium conditions. These comprise, for example, changes in polymer conformation, relaxation times, glass transition temperatures, and all phase transitions under strong confinement, when the film thickness is comparable to the chains' radii of gyration.[20,54−56] We also exclude self-consistent field and density functional theories of inhomogeneous soft matter systems, which are important for modeling diffuse polymer−polymer interfaces.[57,58] Similarly, we will not discuss polyelectrolyte solutions, which play a key role in underwater adhesion; the review by Muthukumar provides an excellent starting point for the interested readers.[59] On the other hand, one feature that is common to all adhesion phenomena is the possibility of scission of the polymer chains. We have already emphasized that this is an important energy dissipation mechanism. Chain breakup is important also for polymer degradation and durability in the natural environment, which is an increasing concern.[60] Below we shall devote ample space to this topic, as we expect it to become an area of significant activity in the coming years, also from a modeling perspective.

The technological classification[2] into structural, elastomer-based, and thermoplastic adhesives is useful also from a theoretical and modeling perspective. The elastomer-based adhesives are soft and have a high degree of compliance, and their elasticity is largely entropic. Many of their properties can be understood in terms of generic coarse-grained models, rooted in polymer physics.[5,8] Hot-melt adhesives based on thermoplastic polymers (polyolefins, polyamides, etc.) and thermosetting resins (e.g., epoxide-based glues) present different theoretical challenges. In these cases, the adhesive films have a large elastic modulus and typically undergo small deformations, until they break up. Stresses within these materials have a predominant enthalpic component, which can be captured at the continuum level by linear elasticity, essentially neglecting their (macro)-molecular nature. At small length scales, they could be simulated using atomistic molecular dynamics (MD). These simulations are possible, but they are still challenging by today's standards (see The Role of Computer Simulations). One key point is that, before computing the mechanical properties of an adhesive layer, one must have a reasonable starting atomistic model for it. This task is not trivial, if we consider the need to account for polymer crystallization,[61−64] the structure equilibration of highly entangled polymers,[65,66] the interactions and changes in polymer conformation at interfaces,[67] or the chemical reactions among the starting monomer units (for the thermosetting resins and cross-linked elastomers).[68−70] Today, many modeling studies of polymers involve the use of computer simulation. However, before embarking on a discussion of current challenges to simulations of polymer adhesion, we present some general ideas arising from theoretical studies.

The effect of preparation conditions on the elastic properties of adhesive polymer layers was modeled by Allegra and co-workers.[71] They developed an equilibrium statistical theory for the shear and elongational moduli of adhesive polymer layers, based on a lattice model of polymer chains forming some covalent bonds with the confining surfaces. These lattice models allow an exact evaluation of the chain partition functions, treating volume interactions at a mean-field level, but accounting for finite chain extensibility. They considered both the case of monodisperse chains forming intersurface bridges (model A) and the case of an infinite chain winding between the surfaces (model B). In model B, the monomers in contact with the surfaces are suddenly "frozen" to model the formation of covalent bonds, in analogy with some theories of rubber vulcanization.[72] The theory predicts that both the elongational and the shear moduli of the adhesive layer decay exponentially with thickness. The former is always larger than the latter, but their ratio converges to unity at increasing thicknesses,[71] as expected for Gaussian statistics.

The behavior at large deformations of soft, rubbery polymer films is of interest for pressure-sensitive adhesives (PSAs).[2,73] In a tack test, the initial detachment of the polymer from the substrate occurs by cavitation of interfacial voids or bubbles. This point corresponds to a sharp maximum in the stress−strain curves. The stress then drops, and there is a broad plateau in the stress−strain curves, during which the polymer fibrils form and stretch up to tens of times the initial film thickness, until complete detachment.[74,75] The viscous stretching of the fibrils is an important energy-dissipation mechanism, bringing the practical work of adhesion well above the thermodynamic value. The polymer must be lightly cross-linked in order to have some solid-like character, suppressing cohesive failure (within the film) in favor of adhesive failure (at the interface with the substrate).

Yamaguchi, Doi, and co-workers[76,77] have developed over the years a fairly comprehensive analytical model for the deformation and breakup of PSAs in tack tests (see also the recent related work by Huang et al.[78]). The most recent version contains the equations for the expansion of the interfacial cavities and their evolution into fibrils. A combination of analytical and numerical solutions provided the full stress−strain curves, which compare favorably with experiments despite some simplifying assumptions. In the conclusions of their latest paper,[79] they explicitly discuss the main shortcoming of the current theoretical model (the maximum in the stress is at relatively small strains) as well as possible improvements to it, such as adopting a nonlinear (visco)elastic constitutive equation for the polymer, removing the assumption of equal size for all the expanding cavities, accounting for the competition between interfacial cavitation, external crack propagation, and bulk cavitation.

Models of Chain Scission. One of the first discussions of the effect of a pulling force on the rate of scission of polymer chains is that of Kauzman and Eyring.[80] In 1940, they attempted to describe the effective viscosity of a sheared polymer film, in which the chains are capable of forming bonds with the confining surfaces and undergo scission when they are deformed beyond their maximum extensibility. It was a bold attempt as polymer science was still in its infancy[1] and the first statistical theories of rubber elasticity were just appearing.[81] Kauzman and

https://doi.org/10.1021/acs.macromol.1c01182
Macromolecules 2021, 54, 10617−10644

Eyring introduced the concept of force-tilted potential energy curve (or, more generally, potential energy surface) for a molecule or polymer chain:[82]

$$V_F(\mathbf{R}_1, ..., \mathbf{R}_N) = V_0(\mathbf{R}_1, ..., \mathbf{R}_N) - \mathbf{F}\cdot(\mathbf{R}_N - \mathbf{R}_1) \quad (16)$$

where V_0 is the unperturbed potential energy surface (Figure 4).

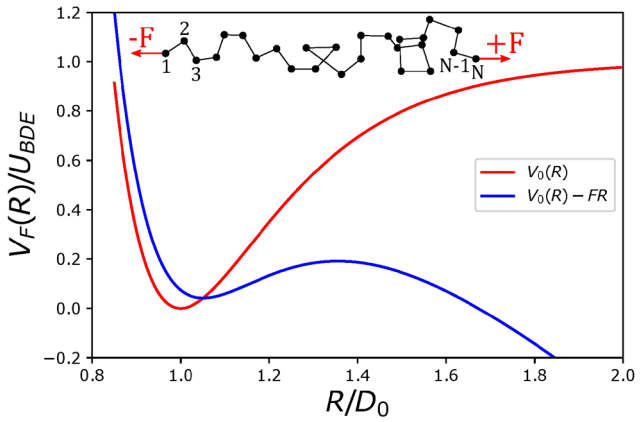

Figure 4. An unperturbed and a force-tilted potential energy curve for the dissociation of a chemical bond. The axes are scaled by the unperturbed equilibrium distance D_0 and the bond dissociation energy U_{BDE}. The inset shows a polymer chain of N beads subject to a pair of pulling forces.

The force **F** is applied, in opposite directions, to the atoms at the ends of the molecule, with coordinates $\mathbf{R}_1$ and $\mathbf{R}_N$ (Figure 4, inset). For a coarse-grained model of a chain molecule (e.g., beads on a string), it is possible to rewrite eq 16 as a sum of individual bond potentials:

$$V_F(\mathbf{R}_1, ..., \mathbf{R}_N) = \sum_{i=1}^{N-1} \{V_{0,i}(D_i) - \mathbf{F}\cdot(\mathbf{R}_{i+1} - \mathbf{R}_i)\} \quad (17)$$

where $V_{0,i}$ is the unperturbed potential for a single bond and $D_i = \|\mathbf{R}_{i+1} - \mathbf{R}_i\|$ is its length). Since then the concept of force-tilted potential energy curve has arisen in a variety of contexts[83,84] and underlies all current work on mechanochemistry, also known as chemomechanics.[85−87] This is depicted schematically in Figure 4, for the simple case of a single bond described by a Morse function. It is now well-established that a force, with the right orientation with respect to its points of application, can produce "unusual" rearrangements within a molecule, opening new reaction channels and synthetic pathways.[88] Today, a great deal of research in polymer mechanochemistry focuses on the synthesis and application of new mechanophores, "weak" bonds that promote chain scission reproducibly under the action of a small force,[89,90] or the design and application of fluorescent probes of chain scission.[91] However, unexpected and useful mechanochemical features may also be embedded in conventional polymers. One example is the force-induced *cis*-to-*trans* isomerization of carbon−carbon double bonds.[92,93] This may play an important role in the toughening of poly(*cis*-1,4-isoprene) (the main component of natural rubber), on top of other well-known mechanisms such as strain-induced crystallization.[52,94]

The "chemistry of bond breaking" has a special role within polymers, because their applications as structural materials often require an ability to withstand large mechanical forces and deformations. Typically, covalent bonds break homolytically under forces that are in the nanonewton range. We point out that chain breakup may occur also in entangled polymer melts and in solutions subject to strong extensional flows,[95−97] a phenomenon that is well-known to polymer scientists but may come as a surprise to physical chemists working on small molecules, where covalent bonds are considered to be indestructible in comparison with other interactions. An important early contribution was that of Lake and Thomas,[49] who developed a model to describe the mechanical toughness of rubber networks.[52] Lake and Thomas measured threshold fracture energies (i.e., at low deformation rates and high temperatures, thus minimizing viscoelastic dissipation) $\Gamma_0 = 50$ J/m^2. Multiplying this value by the typical cross-sectional area of one chain, they concluded that the energy required to break one chain in two is well above 350−400 kJ/mol, the typical dissociation energy of C−C single bonds (U_{BDE}). They reasoned that, instead of being a constant derived from the type of bonds making up the chain, the fracture energy of a chain should be proportional to the number of its chemical bonds or to the number N of statistical segments. [Kuhn segments of length $b = C_\infty l \cos(\theta/2)$, where l is the chemical bond length, θ the angle between successive bonds, and C_∞ Flory's characteristic ratio.[8]] This occurs because a large amount of work is employed to stretch all bonds in the chain and bring them to a near-breaking point. Eventually, only one of them will be broken, and all the excess energy is dissipated as heat.

The Lake−Thomas argument applies both to the fracture of bulk polymers and to adhesion problems, as shown in Figure 5. It

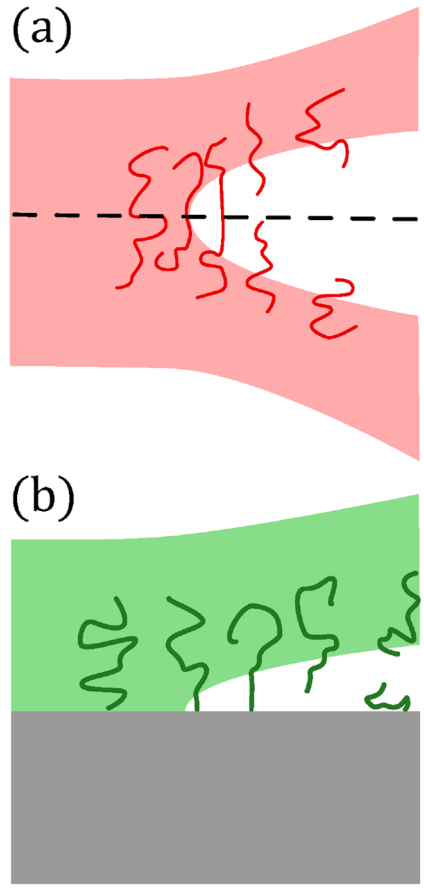

Figure 5. Scheme of the fractures propagating (a) within a polymer or (b) at the interface between a polymer and a rigid substrate.

https://doi.org/10.1021/acs.macromol.1c01182
Macromolecules 2021, 54, 10617−10644

proceeds by considering a plane within the adhesive layer, containing an initial flaw that expands as the fracture proceeds. If Σ is the number density of chains crossing a unit surface, the threshold fracture energy will be

$$\Gamma_0 = \Sigma N U_b \tag{18}$$

assuming that all chains have the same length and contain a single bond type. The U_b energy in eq 18 was originally identified with the unperturbed bond dissociation energy U_{BDE}, but it should be considered an adjustable parameter to take into account the deformation of the bond potential energy produced by the mechanical forces (see again Figure 4). In turn, in a polymer melt or network in which the chains are unperturbed, $\Sigma \propto N^{-1/2}$. Hence, we have

$$\Gamma_0 \sim N^{1/2} U_b \tag{19}$$

showing that the fracture energy increases with the square root of the polymer molecular weight (or of the average molecular weight between the chain entanglements or cross-links). We stress again that eq 19 represents a lower limit on the fracture energy, as a finite crack propagation rate would increase the amount of energy dissipation.

Quantitative application of eqs 18 and 19 to the analysis of the fracture energy of polymer networks and adhesives can be difficult, because the structural heterogeneity which is typical of these systems implies a broad distribution of N values.[98] In recent years, data from single-molecule force spectroscopy experiments (AFM-FS, see the next section on experimental characterization methods) have allowed a detailed comparison with theoretical predictions.[90,99] The force−elongation curves obtained from these experiments can usually be fitted with a modified freely jointed chain model:[100]

$$R = L_0\left[\coth\left(\frac{F}{F_c}\right) - \frac{F_c}{F}\right]\left(1 + \frac{F}{F_s}\right) \tag{20}$$

Here $L_0 = Nb$ is the nominal contour length of the chain, and F_c is a characteristic "conformational" or entropic force ($=k_BT/b$), which typically is of the order of a few piconewtons. The second term in eq 20 accounts for its enthalpic elasticity and includes a characteristic "stretching" or enthalpic force F_s, which typically is of the order of a few nanonewtons (comparable to the forces capable of causing chain scission). The integral of the force−elongation curves, from zero up to the scission distance (R^*)

$$W = \int_0^{R^*} F\,\mathrm{d}R \tag{21}$$

provides the energy stored within the chain at the breaking point. Dividing this by the number of chain bonds, Wang et al.[100] obtained a typical stored energy $U_b \approx 60$ kJ/mol, substantially smaller than U_{BDE} for a C−C bond. There is a subtlety in the last step, because the Kuhn length obtained from fits of the stress−elongation curves with eq 20 may differ appreciably from the conventional Kuhn length, obtained from the unperturbed mean-square end-to-end distance for the same polymer:

$$\langle R^2\rangle_0 = L_0 b = Nb^2 \tag{22}$$

In their paper, Wang et al.[100] stress that U_b should be interpreted as the energy difference between the minima of the force-tiled and unperturbed potential energy curves, as depicted in Figure 4 (*not* the total activation energy for dissociation of the unperturbed or force-tilted bonds). The fact that a relatively small amount of mechanical work is so effective in producing chain dissociation is surprising at first, but it can be justified by recognizing that this work is effectively *coupled to the reaction*, instead of being randomly distributed among the reactant's degrees of freedom.

Polymers are viscoelastic, due to the long relaxation times associated with collective chain motions.[5,40,101] This implies a rate dependence in their mechanical response, which however is neglected in most models of chain scission. One possible justification, apart from the additional mathematical difficulties, is that viscoelastic energy dissipation occurs within the bulk of the polymer, away from the crack tip where chains are broken.[102] Note that this view has been challenged by recent experiments on the fracture of elastomers, showing that many scission events actually occur within the bulk, hundreds of micrometers from the crack tip.[103] The effect of deformation rate was explicitly taken into account by Chaudhury and co-workers, in order to interpret their experiments on adhesion between poly(dimethylsiloxane) (PDMS) networks and functionalized glass surfaces.[104,105] They described the fracture at a polymer−substrate interface with a kinetic model based on the force-dependent rates for bond breaking and formation. Their model builds on the early insights of Kauzman and Eyring[80] and on Schallamach's model of rubber friction.[106] It leads to the following law for the fracture energy, including its dependence on the velocity v of the opening crack, where we have used our previous notation:

$$\Gamma(v) = \Sigma\frac{Nb^2}{6k_BT}\left[\left(\frac{k_BT}{\lambda}\ln\left(\frac{3\lambda\tau}{N^2b^2}v\right)\right)\right]^2 \tag{23}$$

Here, λ is an "activation length" (assumed to be constant, even though the location of the transition state for bond dissociation should depend on the strength of the applied force), and τ is a characteristic relaxation time for the dissociation of a bond:

$$\tau = \frac{h}{k_BT}\exp\left(\frac{U_a}{k_BT}\right) \tag{24}$$

where h is Planck's constant and U_a is an activation energy, which is treated as an adjustable parameter. The expression for $\Gamma(v)$ is consistent with that of Lake and Thomas, at least for the prefactor giving the dependence of the fracture energy on the chain length N (remembering that $\Sigma \propto N^{-1/2}$). Note that eq 23 predicts a logarithmic divergence in $\Gamma(v)$ when $v \to 0$, in disagreement with eq 14, but this limit is never reached in practice.

Experimental data by the same group[104,105] on the rate-dependent adhesion between PDMS and glass surfaces characterized by different chemistries can be fitted according to eq 23. The fits provide an estimate of the relaxation times τ and hence of the activation energies U_a in eq 24. The relaxation times depend on the type of interaction between the elastomer and the substrate. The systems with only weak dispersion interactions are characterized by low adhesion, with a virtually rate-independent fracture energy. This implies a very small relaxation time ($\tau \simeq 1\ \mu$s), with an effective chain length $N = 1$ because the broken "bonds" are those at the interface with the substrate. When the surface chemistry implies stronger hydrogen bonding interactions, the relaxation times increase to 10^4−10^{10} s, depending on the PDMS chain length N. This can be interpreted as an indication that some chain scission occurs also away from the interface, concurrently with the disruption of the

https://doi.org/10.1021/acs.macromol.1c01182
Macromolecules 2021, 54, 10617−10644

interfacial hydrogen-bonding interactions. Finally, when the polymer is chemically grafted to the glass surfaces, the relaxation time increases to about 10^{13} s, implying an activation energy U_a = 151 kJ/mol, which is smaller than the bond dissociation energy of a Si−O bond (U_{BDE} = 454 kJ/mol). There is a similarity with the conclusion reached by Wang et al.[100] on the Lake−Thomas model, even though U_a and U_b represent different quantities. With reference to Figure 4, the first one is the energy difference between the transition state and the minimum on the force-tilted curve, whereas the latter is the energy difference between the minima of the force-tilted and the unperturbed curves.

It is well-known that the viscosity of the medium surrounding the reactants can have an effect on the reaction rates, because it affects their diffusion. This is not included in the transition-state theory, which underlies eq 23, but it can be modeled by Kramers' rate theory.[107,108] For the case of a single particle of mass m undergoing one-dimensional Brownian motion in a potential $V_F(x)$, the probability density $P(x, v, t)$ that the particle is found at position x with velocity v at time t satisfies the Kramers equation:

$$\frac{\partial P(x, v, t)}{\partial t} = \left[v\frac{\partial}{\partial x} + \frac{V_F'(x)}{m}\frac{\partial}{\partial v} + \gamma\left(1 + \frac{\partial}{\partial v} + \frac{k_B T}{m}\frac{\partial^2}{\partial v^2}\right)\right] P(x, v, t) \tag{25}$$

where γ is an effective friction coefficient, proportional to the local viscosity η. According to the Stokes approximation, $\gamma = 6\pi\eta a/m$ for a particle of radius a. $V_F'(x)$ is the gradient of the potential energy, which depends on the applied force F. Steady-state solutions to this one-dimensional problem can be obtained analytically in the low-damping and large-damping limits, respectively corresponding to small and large γ values, but also numerically.[109] Physically, the steady-state condition corresponds to a situation where new bonds are constantly brought into the stretched state and broken by a fracture propagating at constant velocity. The rate can be identified with the flux j of bonds that overcome the dissociation barrier (located at $x = x_b$, which depends on the applied force F), normalized by the total number of bonds n before dissociation (neglecting the reformation of bonds following dissociation):

$$k(F) = \frac{j}{n} = \frac{\int_{-\infty}^{+\infty} \mathrm{d}v v P(x_b, v)}{\int_{-\infty}^{x_b} \mathrm{d}x \int_{-\infty}^{+\infty} \mathrm{d}v P(x, v)} \tag{26}$$

where the dependence on time has disappeared from $P(x, v, t)$ because of the steady-state assumption. Let us denote by ω_1 and ω_2 the angular frequencies describing the curvature of the potential energy at the minimum and at the transition state [i.e., $\omega_1 = \sqrt{V_F''(x_m)/m}$ and $\omega_2 = \sqrt{-V_F''(x_b)/m}$]. Interpolating between the rates obtained from the small- and large-damping solutions to eq 25, the rate may be approximately written as[105,108]

$$k(F) = \left[\frac{\omega_2}{\sqrt{\frac{\gamma^2}{4} + \omega_2^2} - \frac{\gamma}{2}} + \frac{\omega_1 k_B T}{2\pi\gamma U_a(F)}\right]^{-1} \frac{\omega_1}{2\pi} \mathrm{e}^{-U_a(F)/k_B T} \tag{27}$$

(note that also the ω_i's depend on F). In this expression, the term outside the parentheses is the rate from transition state theory $[k_{TST}(F)]$. The prefactor is a correction depending on the viscosity of the medium through γ. This can reduce $k_{TST}(F)$ by up to 1 order of magnitude, both in the small-γ and in the large-γ limits. Hence, it seems desirable to have a good estimate of the effective viscosity of the chains undergoing scission. We point out that a large fraction of the viscosity may arise from local conformational effects, through the energetic barrier to conformational transitions that occur at high deformation rates ("internal viscosity").[110,111] PDMS—the polymer used in the experiments by Chaudhury's group—is very flexible and has a small internal viscosity,[112] so that the dynamics should not be too different from that based on transition state theory. Nonetheless, re-evaluation of the PDMS bond scission data based on eq 27 leads to a new estimate of the activation energy, at 216 kJ/mol instead of 151 kJ/mol (still significantly lower that U_{BDE} = 454 kJ/mol).[105]

A further refinement to the theory of chain scission in a viscous medium follows by adopting the multidimensional Kramers equation.[113] In this case, the equation describes the evolution of a multivariate probability distribution $P(\{x_i, v_i\}_{i=1}^N, t)$, where N is the number of breakable links within a chain.[114,115] Within this framework, it is possible to investigate the rate constants for breaking bond i under the action of a force F $[k_i(F)]$ and the probabilities that the chain is broken at a given bond $[P_i(F)]$. These should be related as follows:[116]

$$P_i(F) = \frac{k_i(F)}{k(F)} \tag{28}$$

where the denominator is the overall rate of breakup (at any bond):

$$k(F) = \sum_{j=1}^{N} k_j(F) \tag{29}$$

Ghosh et al.[115] obtained analytical expressions for the rates and probabilities and compared them with the results of MD simulations for a coarse-grained chain model with a Morse potential for each bond. When one end of the chain is tethered to a fixed point (e.g., bonded to a rigid surface) and the other end is subject to a constant pulling force, they found that the probability of breakage increases monotonically from the tethering point to the pulling point. When both ends are subject to opposite pulling forces, the central bonds are less likely to break than those at the ends, but this difference tends to vanish when the pulling forces become weaker.[117] The anharmonicity of the bond potential and the bending stiffness are also important, as they both tend to enhance the probability of chain scission at the ends.[118] Although this is clearly a highly simplified model, there seems to be a lesson for more complex adhesion problems. Other things being equal, when pulling on a film in which the chains are chemically bonded to a rigid substrate, it would be more likely to break the chain bonds away from the substrate.

Further investigation of these issues is desirable, for example with respect to the effect of local stereochemistry and torsional barriers on bond scission. It is not clear if the main aspects of it can be captured by coarse-grained models, which may also admit analytical solutions, or if it will be necessary to adopt fully atomistic MD simulations. For example, it would be interesting to compare the ultimate mechanical properties of single chains with different tacticities, which can have very different

https://doi.org/10.1021/acs.macromol.1c01182
Macromolecules 2021, 54, 10617−10644

conformational properties.[119] The size of torsional barriers affects the frictional forces between polymer surfaces,[120] as was shown by a model for the internal viscosity of the chains.[121] Given sufficient statistics with a large number of independent repetitions, nonequilibrium MD simulations of single-chain stretching can also yield their free energy profiles through the celebrated Jarzynski equality.[122] The comparison between single-molecule pulling experiments (AFM-FS) and MD simulations is an area where we expect to see substantial work in the future, aiming at a quantitative agreement both in situations where there is simple unfolding of the polymer conformations, and in those in which there is mechanochemical activation and breaking of covalent bonds (see, for example, ref 123 and references therein). Computer simulations can be applied also to the fracture and adhesive failure in many-chain systems, and we turn to them in the following subsection.

The Role of Computer Simulations. Our discussion of simulations will be largely restricted to the MD method. Its unique advantage, which sets it apart from other theoretical and computational approaches, is the possibility to deal with fast, out-of-equilibrium, and nonlinear phenomena.[124−126] These are exactly the type of problems which arise in adhesion, especially close to interfaces where local stresses and strains can be large, mechanical energy is dissipated as heat, and chemical bonds might be broken. Of course, it is important to be aware also of the current limitations of the method. These are mainly determined by the accessible time- and length-scales, the required accuracy in representing chemical and physical interactions among the atoms, and the treatment of the system's interaction with the environment. Below we discuss these issues and present application examples from the recent literature. In doing so, we will also identify areas where methodological developments would make a significant difference.

First-principles MD simulations, which are based on on-the-fly quantum mechanical calculations of the forces among the atoms,[127] require major computational resources. They can be applied to virtually any chemical system, typically using versions of density functional theory[128] whose reliability has been extensively tested and refined over the years. Because of progress in hardware and software (see Kühne et al.,[129] for example) they can currently deal with systems containing 10^2-10^3 atoms, over short time scales (well below 1 ns). Although this might appear to be a severe limitation, these methods can be usefully applied to the interaction of small molecules with model surfaces (e.g., catechol on hydrated silica)[130,131] or to the force-induced scission of short polymer chains.[87,132] Such simulations can be of interest in their own right, or as a way of validating the empirical force fields that are applicable to much larger systems.[133,134] We also point out that, despite its many successes and popularity, there should still be some interest in testing the performance of density functional theory in the description of extreme bond-breaking situations, using for example electronic structure methods based on suitably correlated wave functions.[135]

Due to the cost of first-principles MD simulations, most computational studies of polymer adhesion have been and will be done with empirical potential energy functions. Today or in the near future, for someone with "reasonable" access to supercomputers or clusters with graphical processing units, it should feasible to simulate in atomistic detail systems containing up to 10^6 atoms (roughly equivalent to a volume of 10^4 nm^3), for time scales up to 10^{-6} s. The required computational power scales linearly with the simulation time and, for systems without long-range electrostatic interactions (e.g., hydrocarbons), also with the system size.[136] This means that longer simulations can be traded for smaller system sizes, and vice versa. One important stumbling block for atomistic MD simulations of adhesion phenomena is the difficulty of producing realistic models of the surfaces and the fact that the force fields for organic and inorganic materials (e.g., the polymer and the substrate) may not be compatible with each other.[131] Luckily, the situation is improving from this point of view; for example, see the work of Emami et al.[137] on silica surfaces, which has been employed to derive a coarse-grained model for silica−rubber interfaces.[138] The conventional atomistic force fields for polymers, organic materials, and biomolecules[139] are restricted to a fixed topology, meaning that chemical bonds are assigned *a priori* and can neither be broken nor formed during a simulation. Several "reactive" force fields have been developed over the last 20 years, wherein the potential energy functions depend on empirical bond orders that are computed at every new atomic configuration. The LAMMPS code[136] allows simulations with several reactive potentials, including ReaxFF,[140] AIREBO,[141] AIREBO-M,[142] and COMB.[143] These reactive force fields are heavily parametrized, and they may be restricted to a few elements. Their transferability to different thermodynamic states is not guaranteed and should be checked on a case-by-case basis. Even more recently, new impulse has come from potential functions based on machine learning,[144,145] leveraging on extensive sets of curated *ab initio* electronic structure data.[146] Of course, the power and additional flexibility of the newer force fields comes at a price, so that simulations based on them are 1 or 2 orders of magnitude costlier than those with a conventional one.[147]

As an example of relevant atomistic MD simulation, we mention some recent work on structural adhesives based on thermosetting resins. The critical step for the simulation of these systems is the initial preparation of a tightly cross-linked network, starting from the monomers.[68] This step affects all the thermophysical properties of the resulting models, such as the glass transition temperature, thermal expansion coefficient, elastic moduli, and yield stress. Even when using a reactive force field[148] or a hybrid quantum chemical model,[149] the cross-linking reaction cannot be simulated by "brute force" integration of the MD equations of motion because of the extreme disparity between the experimental and the computationally accessible time scales. Rather, the cross-linking reaction must be performed by a combination of probabilistic bond creation and structure relaxation steps.[150−152] Once this is done, a simulation of mechanical deformation with a reactive force field may describe also the ultimate mechanical properties.[153]

Near-atomistic simulation of the mechanics of a thermoplastic semicrystalline polymer (polyethylene) has been carried out by Rutledge and co-workers.[64,154] These employed one united-atom per CH_2 group and excluded chain scission. Again, the most critical part of these simulations is probably the initial preparation of the system, with a correct distribution of the chains among the crystalline and amorphous domains. This can be achieved by special purpose Monte Carlo moves. The subsequent simulations of the mechanical deformation highlighted plastic rearrangements, melting and recrystallization within the crystalline domains, as well as the contribution of entanglements to the mechanical properties of the amorphous domains.[64] Simulations of glassy polyethylene nanofibers were originally intended to study the properties of electrospun nanofibers, but they could equally apply to be fibrils that develop in polymer fracture.[154] These simulations demonstrated a

https://doi.org/10.1021/acs.macromol.1c01182
Macromolecules 2021, 54, 10617−10644

significant dependence of the yield stress of the fiber diameter, the typical values being approximately half of those of the bulk amorphous polymer.

The adoption of coarse-grained models produces additional gains over atomistic ones, by reducing the number of atoms and by allowing longer time steps in the integration of the equations of motion.[155,156] The gains can be roughly quantified at 1 order of magnitude, in both the accessible system size and time scales. The potential parameters describing the interactions among the coarse-grained units can be derived from those of the underlying atomistic model, using criteria such as the reproduction of certain structural features (e.g., distributions of bond lengths and angles) or the potential of mean force between different groups of atoms.[157] In principle, it is also possible to combine atomistic and coarse-grained models within the same simulation in an adaptive way, keeping the atomistic—or even quantum mechanical—details only for the most critical parts of the system, such as the interface or the regions subject to the largest stresses.[158,159] For aqueous systems, such as hydrogels and adhesive proteins, another possible way of achieving higher efficiency consists of the adoption of an implicit solvent model. When studying the mechanics of adhesion, such as an aqueous protein layer bridging to surfaces, in addition to "rescaling" the nonbonded interactions among the solute atoms[139] it seems important to account properly also for hydrodynamic effects, because the solvent can be quite literally "sucked in" and "squeezed out" by the motion of the surfaces. The Lattice Boltzmann method is a good candidate for this purpose.[160] More generally, the simulation of adhesion problems should benefit from the development of ways of coupling the molecular scale with the macroscopic one, for example through concurrent MD and finite-element simulations.[161,162] These methods are typical examples of multiscale approaches, but they may be viewed also as generalizations and improvements of the thermostats and barostats that are used in conventional equilibrium and nonequilibrium MD simulations.[124−126]

The dynamics of a coarse-grained model is usually faster than that of the underlying atomistic one, reflecting a smoother potential energy landscape.[163] This is usually considered an advantage, as is leads to faster relaxation (of the stress, the end-to-end distance of the chains, etc.) and to improved sampling of the system's configurations, but it might be a disadvantage if the aim is to probe the nonequilibrium response to a perturbation, such as a mechanical deformation. The possibility of recovering reliable dynamical and mechanical properties from coarse-grained simulations is not yet fully established and should be pursued also in connection to adhesion problems. One recent encouraging example comes from the application of the "energy renormalization" coarse-graining approach to a biomimetic copolymer adhesive, poly(catechol-styrene).[164] One specific feature of this method is that the nonbonded potentials are allowed to be temperature-dependent, to compensate for the loss in microscopic degrees of freedom implicit in coarse-graining. This allowed the authors to reproduce the dependence of both dynamical and mechanical properties of the underlying atomistic model (diffusion coefficients, segmental relaxation, elastic moduli, etc.) over a broad range of temperatures and compositions (100−500 K and 0−50% in cathecol content). The adhesive properties to a substrate, which depend also on the interfacial free energies, were not tested, but presumably they will be in the near future. Note that this model does not allow bond breaking. Instead, a coarse-grained model for epoxy resins incorporating the possibility of bond breaking was developed by Yang et al.,[165] building on previous work by Tsige and Stevens.[166] In this case, the coarse-grained potentials were not derived from atomistic simulation but were obtained by direct comparison of the calculated thermophysical properties with target experimental values. The model allowed large-scale MD simulations of the tensile behavior and failure of the resin.[167] The results are encouraging but, to our knowledge, there is still no established criterion for deriving the bond scission parameters of a coarse-grained model from atomistic—possibly quantum mechanical—simulations. Whether this can be achieved is an open question.

Several interesting computational studies of polymer adhesion have been carried out with modifications of the Kremer−Grest (KG) bead-and-spring model.[169] This is a physics-based coarse-grained model, which does not attempt to reproduce the properties of any specific polymer, although it can be mapped onto a wide selection of commodity polymers in a way that reproduces some of their large-scale properties in the molten state (e.g., the Kuhn and packing lengths) after inclusion of a bond-bending term.[170] With additional interchain bonds that mimic vulcanization, it has been used extensively to test statistical theories of rubber networks,[8,98,171] including their aging[172] and their mechanical reinforcement by solid nanoparticles.[173,174] Note that neither the original nor the modified versions of KG can be applied "as such" to simulate adhesion. The main reason is that the bead−bead interactions are represented by a truncated variant of the Lennard-Jones potential that renders them purely repulsive. This can easily be fixed by including the attractive tail of the Lennard-Jones potential.[175] Once this is done, the KG model exhibits also a glass-transition temperature, but it does not undergo crystallization because of the high chain flexibility.[55] Another important feature of the original KG model is the fact that bonds have a finite extensibility, designed to preserve interchain entanglements.[169] Bonds described by these potentials can never be broken, unless they are explicitly "instructed" to do so (by special purpose Monte Carlo moves, for example).[172] In some cases, the original bond potentials were used as such in simulations of the mechanical deformation of adhesives, thus preventing the possibility of chain scission.[168,176−180] This possibility was introduced in the form of a quartic potential with a bond-breaking barrier approximately equal to 20ϵ, where ϵ is the energy of the nonbonded Lennard-Jones interactions.[181] This model was used to simulate the interfacial fracture of polymer networks on solid surfaces,[181] the competition between chain pullout and scission at adhesive polymer interfaces,[182,183] and the fracture of polymer networks and gels.[184,185] A similar model was used in Monte Carlo simulations of dissipation and elastic recovery in networks containing sacrificial but healable bonds, subject to cyclic loading.[186] Last but not least, we mention our own work on polymers between chemically heterogeneous surfaces, which highlighted a systematic dependence of the equilibrium dynamics and the adhesive forces on the morphology of the surfaces (see Figure 6).[168,180]

Coarse-grained bead-and-spring models were used extensively and very effectively by Robbins and co-workers, not just for polymer fracture and adhesion problems, but also for gaining physical insights into contact mechanics, friction, lubrication and wear.[176,183,187−192] These studies can still be an inspiration for future work in this area, aiming for example at replicating them with more realistic atomistic models.

Surface Roughness and Textures. All solid materials, including polymers, show some surface roughness, and this is

https://doi.org/10.1021/acs.macromol.1c01182
Macromolecules 2021, 54, 10617−10644

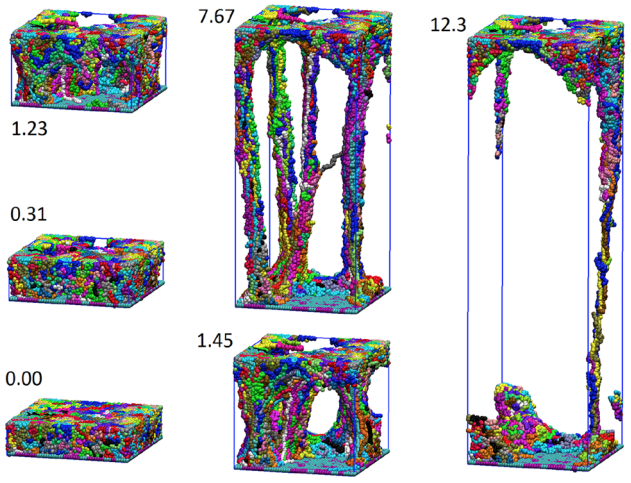

Figure 6. Coarse-grained simulations of the deformation and breakup of a rubbery polymer film between two chemically heterogeneous surfaces. The strain values (ϵ_{zz}, see eq 6) are reported next to each snapshot. The upper surface has been deleted for clarity. Reproduced with permission from ref 168. Copyright 2021 American Chemical Society.

known to have a strong effect on adhesion. On the one hand, polymer adhesives that are applied as fluids before curing adhere more strongly to rough surfaces after curing, because the true area of a rough surface is larger than its nominal (projected) area. On the other hand, roughness frustrates adhesion between elastic materials by reducing their real contact area A_c to a small fraction of the apparent (or projected) contact area A_a. This is the main reason why adhesion is rarely observed for hard polymers,[28] whereas softer polymers that are able to conform to surface asperities show an increased adhesion. For example, a root-mean-square roughness as small as one nanometer significantly reduces the adhesion of glassy polymers such as polystyrene, particularly in shear adhesion tests (see also Figure 7a below). A roughness of just a few nanometers is sufficient to remove adhesion for relatively stiff cross-linked elastomers,[193,194] whereas a few micrometers are necessary to reduce by 1 order of magnitude the adhesion of soft rubbers and gels.[195]

Early theories assumed that roughness could be described as a surface distribution of round asperities with an average radius of curvature and different heights, progressively coming into contact as the applied normal load increases.[195−197] Theoretical predictions were expressed as a function of statistical quantifiers such as the root-mean-square roughness and average radius and slope of the surface asperities. Although such models are still used to study particular types of roughness, elasticity, adhesive interfaces, and load conditions, their applicability is inherently limited. The critical point is that most natural and engineering materials display a multiscale surface topography that is not captured by simple asperity models. Namely, roughness is characterized by the power density spectrum of the surface topography, such that the amplitude h of the roughness component with wavelength λ decays as λ decreases toward the nanoscale, often following the typical power-law decay of self-affine (fractal) structures.[28,198,199] This topography is better described as small asperities added onto large asperities, which are on top of even larger asperities, and so on. Conventional statistical quantifiers show a dependency on the scale and resolution of the measuring technique and therefore do not correctly characterize the topography.[199] Adhesion theories have evolved to incorporate approximate models with fractal roughness.[199,200] Roughness, however, can take many different forms, some of which are irreducible to a single number or fractal exponent.[28] It is only recently that Persson and collaborators have developed a comprehensive continuum mechanics theory, allowing quantitative calculations of adhesive forces as a function of experimental roughness spectra with arbitrary complexity.[201−204] Achieving complete (conformal) contact between two rough elastic materials requires deforming at least one of the materials and storing elastic energy near the contact interface. Therefore, complete contact is obtained when the gain in adhesive energy exceeds the stored elastic energy, or the materials are pushed against each other under a sufficiently large normal load. For a soft material in contact with a hard rough surface under zero applied load, the theory provides a scale-dependent criterion for complete contact: $h/\lambda \leq (l/\lambda)^{1/2}$, where l is the elasto-adhesive length (eq 10). For fractal rough surfaces, this criterion implies that complete contact occurs up to a

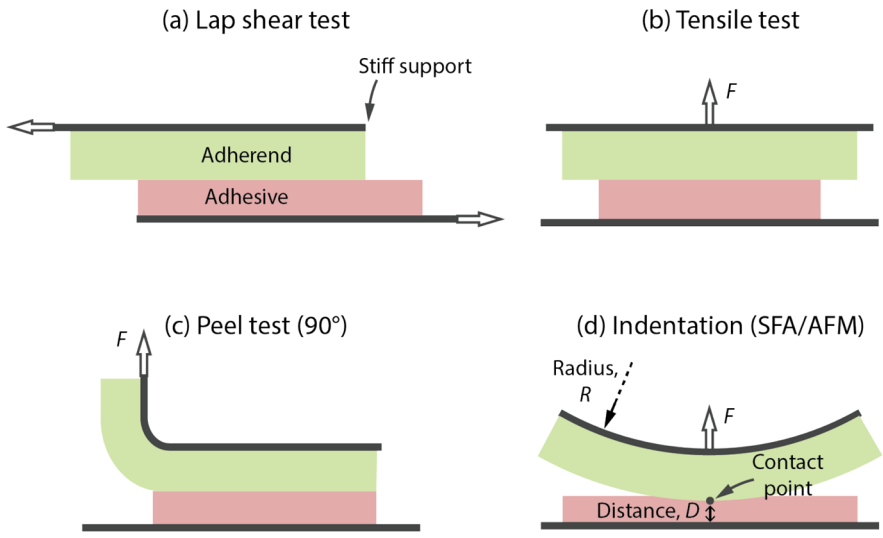

Figure 7. Mechanical tests for measuring the adhesion and mechanical properties of a polymer material at the macroscopic scale. The adherend can be made of the same material as the adhesive to study cohesion.

https://doi.org/10.1021/acs.macromol.1c01182
Macromolecules 2021, 54, 10617−10644

maximum wavelength. Roughness components with larger wavelengths create taller surface peaks and deeper valleys, and the soft material covers these peaks without filling the valleys. In parallel with theoretical developments, calculations of the total contact area A_c as a function of the normal force F, multiscale structure of the contact interface, stress distribution over the contact area, and role of plastic versus elastic deformation have become feasible.[205−208]

Accurate roughness measurements can now be obtained combining multiple topographic techniques with different resolutions, such as optical and stylus profilometries and atomic force (AFM) and electron microscopies.[209,210] On the other hand, measuring A_c as a function of F (e.g., by electrical and thermal contact resistivity measurements) and resolving *in situ* its multiscale structure with optical microscopy, fluorescent markers, interferometry, and acoustic waves is an ongoing challenge, not least because the contact area is buried beneath solid materials and therefore inaccessible to most high-resolution imaging techniques (see also Buried Polymer Interfaces).[200,211,212] Understanding roughness effects on adhesion, sealing, friction, and wear is a lively research area, where experiments and theory are rapidly converging. For example, Dhinojawala and co-workers recently measured the adhesion force of a PDMS elastomer on diamond surfaces with different roughness, showing a good agreement with the force calculated using Persson's theory of rough surface adhesion.[210] We hope to see more comprehensive studies of this sort in the future, extending the comparison of theory, simulations, and experiment to situations with high-energy, strongly interacting interfaces. Current microfabrication techniques allow the production of surface textures and topographic patterns with submicrometer resolution, which can be used to engineer surfaces with tailored adhesive properties. Notably, a growing research effort is aimed at replicating the efficient reversible adhesion obtained on dry surfaces by biological organisms such as the gecko, relying on a hierarchical multiscale organization of surface protrusions.[213−215]

Multiscale Characterization of Polymer Adhesion. The experimental study of polymer adhesion extends over multiple length and time scales, mirroring the theoretical investigations. While the macroscopic aspects of polymer adhesion can be measured with relatively simple experimental techniques, the characterization of polymer interactions at the molecular and submolecular scale calls for advanced experimental techniques that are at the cutting edge of current nanotechnology.

At the macroscopic scale, the adhesive performance of a polymer material can be evaluated using standardized mechanical tests such as the lap shear test, tensile "tack" tests, and peel test (Figure 7a−c). The International Organization for Standardization (www.iso.org) and American Society for Testing and Materials (www.astm.org) provide measurement guidelines and protocols for a variety of polymer materials and applications. These methods quantify the resistance of an adhesive film as a mechanical force that varies as a function of material deformation. The force generated by the material is opposed to the deformation and decreases rapidly. The mechanical test typically addresses different macroscopic properties of the polymer material. Namely, linear elasticity, nonreversible plastic deformation, and failure are obtained by continuously increasing the amount of deformation, providing measurements of the elastic constants (see again eq 5), strength (yield point), and toughness (fracture resistance).

Despite their practical usefulness, the standardized tests have a limited ability to investigate polymer adhesion at the microscopic scale. The sample dimensions and mechanical testing devices typically are much larger than the size of a polymer molecule, which ranges from 1 to 100 nm. For example, the thickness of the polymer film typically exceeds 100 μm, and sample deformations are resolved at a length scale of a few micrometers at best. Therefore, the standard tests probe the mechanical response of large sample volumes, extended interface areas, and large numbers of polymer molecules, providing a macroscopic average of the different forces generated by the various molecular structures and mechanisms in the polymer film (Figure 2). In particular, it is difficult to discriminate between adhesive polymer interactions at the interface with the adherent and cohesive interactions between polymer molecules.

Nanoscale Force Measurements. Since the end of the 1970s, a few experimental techniques have appeared that are able to directly measure the nanoscale deformations and small forces generated by polymer monolayers and even single molecules, namely, the surface forces apparatus (SFA),[216] AFM with force spectroscopy (AFM-FS),[90,217] optical tweezers,[218−220] and magnetic tweezers.[219] The measured force F originates from a single contact point between two solid surfaces shaped as crossed cylinders (SFA), a sphere and a plane (AFM), or two spheres (optical and magnetic tweezers). In all cases, the surface geometry around the contact point is or can be approximated as a sphere of radius R (more generally, an ellipsoid) at a separation distance D from a plane (see Figure 7d and the JKR geometry in Figure 3b). Adhesion is typically measured by approaching and then retracting the surfaces. This geometry eliminates the uncertainty on the number and curvature of contact points that affects the interpretation of adhesion measurements on planar films and surfaces (see the tensile test in Figure 7b and compare it with Figure 3a).

SFA and AFM-FS are the most widely used of the previous techniques. One surface is attached to a rigid support, while the other is attached to the free end of an elastic cantilever of known elastic constant k, whose fixed end is displaced using precision actuators at a known speed u. SFA and AFM-FS are complementary in terms of the number of probed molecules, time scales, and force sensitivity.

In the SFA, the crossed cylinders have radius R = 1−2 cm. When pressed against each other, they create a circular contact area with a diameter exceeding the size of a polymer chain, thereby probing the mechanical response of a large number of them. The cylinders usually are made of smooth cleaved muscovite mica or noble metals (possibly stripped from a mica template to reduce roughness). The surface can be modified, for example, by exposure to reactive plasma or by coating with a self-assembled monolayer, to tune chemical−physical properties such as surface charge, polarity, and roughness. The polymer is deposited on one of the surfaces to measure the adhesion force with the other surface, or on both surfaces to measure the polymer cohesion force. Near-equilibrium testing conditions are obtained by displacing the SFA surfaces at slow uniform speeds u of a few nm/s or in a step-like motion, allowing up to a few hours for relaxation. The distance D is directly measured with a resolution better than 1 nm using an optical interference technique,[221] while force variations ΔF are determined with a sensitivity of 0.1 μN.

The SFA played a pivotal role in the study of polymer interactions in the 1980s, providing the first direct measurement

https://doi.org/10.1021/acs.macromol.1c01182
Macromolecules 2021, 54, 10617−10644

of the surface forces generated by polymer monolayers.[222] SFA experiments on adsorbed layers of homopolymers[222−226] and brush-like layers of grafted diblock (AB)[227−230] and triblock (ABA)[231,232] copolymer have helped establish the current understanding of polymer nanomechanics and technologies to control surface and colloidal interactions. In particular, colloidal dispersions are often stabilized against flocculation by coating the colloid particles with an antiadhesive polymer layer that generates a repulsive osmotic force at contact with another particle.[15] Yet, SFA experiments proved that in some cases an adsorbed polymer molecule can also bind to the surface of another particle, creating an adhesive polymer "bridge" (Figure 2).[224,225] Another example is provided by mucin glycoproteins that coat, lubricate, and protect many surfaces of the human body, including the oral cavity, gastro-intestinal and reproductive tracts, and articular joints. Mucins have a telechelic ABA structure, where the B block is densely coated with charged and hydrophilic sugar providing an antiadhesive function, whereas the A blocks can bind to each other and to the underlying tissue. Mucins can form dense brushes by attaching to a solid substrate with both A blocks, forming "loops", or one block, forming "tails" (Figure 2), preventing adhesion in both cases. Yet, when the mucin lubricin was allowed to attach its A domains to both surfaces of the SFA simultaneously, the bridging produced strong and tough adhesion.[233] Although bridging may destabilize the antiadhesive properties of polymer coatings, it also gives an interesting parameter for tuning and actively controlling surface interactions. In this respect, it is revealing that bridging interactions play an important role in cell recognition and adhesion.[234−236] Cells are indeed biological "colloids" that use membrane-tethered proteins to interact with other cells and attach specific ligands to their membrane.

The focus of SFA studies has gradually shifted toward charged water-compatible polymers such as polyelectrolytes, polysaccharides, and proteins, which are one level of complexity above neutral homopolymers and block copolymers and are of great interest for medical, biomimetic, and environmentally friendly applications. Brush-like films of end-tethered polyelectrolytes have been extensively studied for their ability to reduce surface adhesion and friction in aqueous solutions.[237−240] Charged polyelectrolytes, however, can also generate adhesion at contact with oppositely charged surfaces[241] and switch from repulsion to adhesion in response to changes in ionic composition[242,243]

The SFA has been a key experimental tool to elucidate the underwater adhesion provided by proteins of aquatic organisms and replicated with bioinspired synthetic polymers, discussed in the last section of this Perspective.

Single-Molecule Mechanics. In the AFM-FS technique, a force-sensing probe is attached to the end of a microfabricated cantilever with a known elastic constant in the range of 0.01−1.0 N/m.[217] A laser beam is typically used to detect subnanometer cantilever deflections, corresponding to mechanical forces in the range of 10−1000 pN.[90] The cantilever can reach very large speeds, $u > 100$ nm/s (Figure 7), while the data acquisition rate typically exceeds 1 kHz. Therefore, AFM-FS is more suited than SFA to study force generation in fast dynamical regimes. On the other hand, static force measurements are difficult to obtain, because the surface distance D (Figure 7d) is subject to thermal and mechanical drifts that cannot be directly measured. The AFM probe generally is the rounded tip of a microfabricated cone or pyramid with a typical end radius R of about 10 nm.[217] The radius can be increased up to a few hundred micrometers by attaching a colloidal sphere to the end of the force-measuring cantilever.[244] The diameter of the contact area between the colloidal probe and the surface is much smaller than in the SFA. In both cases, however, the contact area is much larger than the size of a single polymer, and force measurements on polymer films and interfaces probe the collective mechanical response of a large number of polymer molecules.

Although colloidal-probe AFM-FS considerably expands the force sensitivity, speed, and range of materials that can be tested compared to the SFA, the mechanisms of force generation are essentially the same. Readers interested in colloidal probe AFM-FS will find an excellent review in ref 217. Here we highlight that AFM-FS is able to probe the mechanical response of *one* polymer chain and even single molecular bonds, gaining a fundamentally different perspective on polymer mechanics. The chain is typically stretched using a sharp nanoscale AFM tip. The chain is a portion of polymer molecule that bridges the probe and surface and generates an attractive force when stretched (Figure 2). The typical force sensitivity of the AFM cantilever is of the order of 10 pN and is comparable to the average force acting on a chain in a highly stretched polymer.[90] Although optical and magnetic tweezers provide a better force sensitivity, the AFM offers the key advantages that the polymer morphology can be imaged with subnanometer resolution before and after force measurement, and the polymer environment can be changed from gas or vacuum to a liquid solvent. Single-molecule FS has been reviewed many times,[90,245−247] and here we have selected a few key results.

Single-molecule AFM-FS experiments are able to test the elasticity of a single chain, i.e., the force necessary to keep two units of the same chain at a certain distance. The force−distance relationship is nonlinear and can be fitted with a modified version of one of the classical models of chain elasticity, such as the freely rotating chain, freely jointed chain, or worm-like chain.[8] The modified models include the enthalpic elasticity of small deformations of bond length and bond angle caused by strong chain elongations (e.g., see eq 20) and can be obtained with *ab initio* quantum mechanical calculations in vacuum. They can be fitted to experimental force−distance curves obtained in nonpolar solvents for broad classes of polymers that can be classified according to their backbone: simple C−C backbone such as poly(ethylene) and poly(styrene);[248] C−C−O backbone such as poly(ethylene glycol); polysaccharides with rigid sugar units, such as cellulose, amylose, or chitosan;[249] single-stranded DNA;[250] proteins and polypeptides.[251] Perhaps less intuitively, the steric hindrance between side groups of moderate size, such as the aromatic rings of polystyrene or residues in proteins, have a negligible effect on chain mechanics in nonpolar solvents.[90] On the other hand, water deeply affects the single-chain mechanics of both hydrophilic polymers, such as PEG or single-stranded DNA, and hydrophobic polymers such as PS. In particular, hydrophilic polymers appear stiffer in water, because an additional energy of the order k_BT per unit segment is required to rearrange water molecules around the polymer chain during elongation.[90]

Single-molecule FS is uniquely suited to study chain scission and, in general, structural transitions in stretched polymer molecules. Classical examples include antibody−antigen[252] and ligand−receptor complexes,[253] as well as covalent bonds.[254] Both the energetics and kinetics of the transition (and its inverse) contribute to the mechanical response and can be characterized by modeling the protein domain as a two-state system, as in Bell−Evans theory.[83,84,255,256]

https://doi.org/10.1021/acs.macromol.1c01182
Macromolecules 2021, 54, 10617−10644

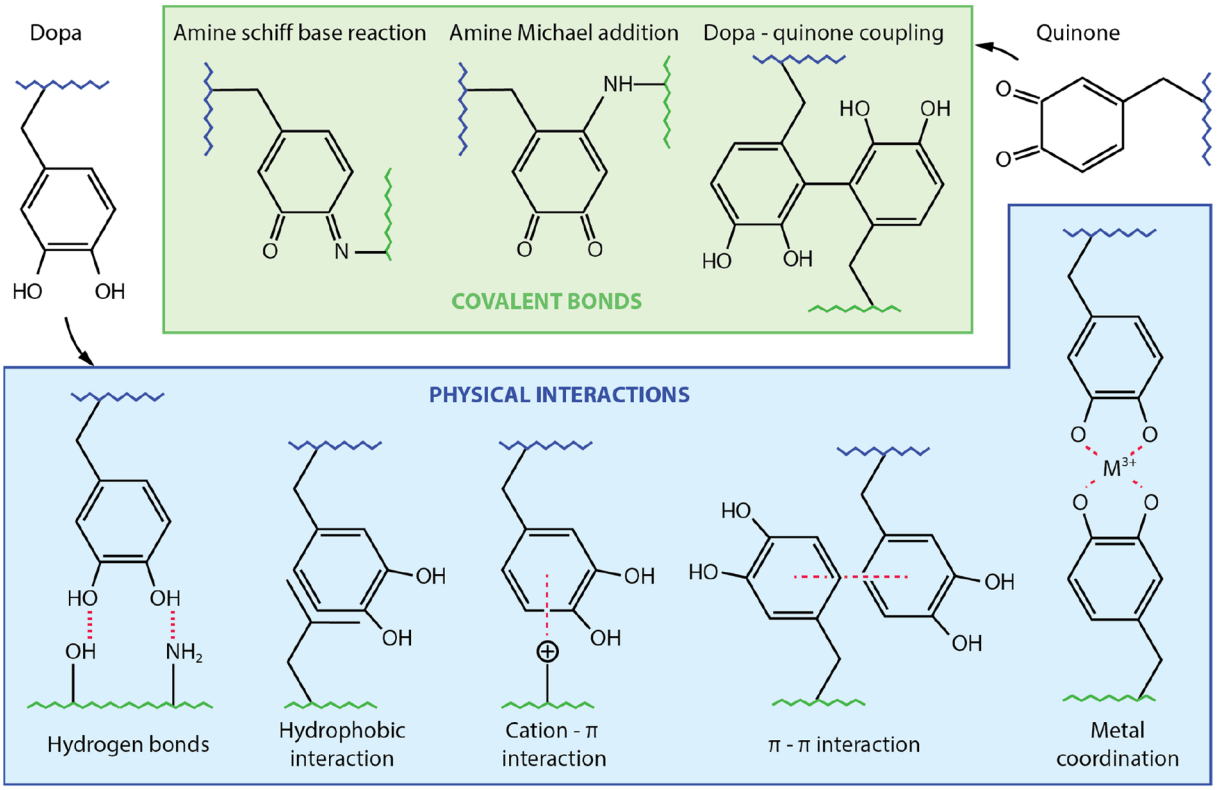

Figure 8. Physical interactions involving the amino acid Dopa, obtained by hydroxylation of tyrosine, and covalent bonds formed after oxidation of the hydroquinone moiety into quinone.

In particular, AFM-FS has been used to quantify surface bonds formed by specific moieties used in polymer adhesives. Two examples are the uncommon aromatic amino acid dihydroxyphenylalanine (Dopa),[255] used by mussels to bind proteins to a variety of surfaces (see Figure 8 and Wet Polymer Adhesives),[46,257] and the short amino acid sequences containing the anionic phosphorylated serine, which is common in calcium-binding adhesive proteins found in mineralized human tissues such as bone. Moreover, single-molecule AFM-FS has been extensively used to characterize the force-induced unfolding of protein domains.[245,247] In addition to their relevance for protein biochemistry, these processes provide an effective way to repeatedly dissipate large amounts of energy in polymer adhesives (Figure 2).[258−261]

Structural transitions have been observed also in non-biological polymers.[90] One striking example is the *cis*-to-*trans* isomerization in chains comprising carbon−carbon double bonds within the backbone.[92,93] Complementary to force-induced transitions, forces can be generated by a single chain and measured by AFM-FS in response to external non-mechanical stimuli. A particularly vivid example is provided by polymers with an azobenzene backbone that can be switched to a *trans* or *cis* state by irradiation with visible or UV light, respectively. Light-induced *trans*-to-*cis* isomerization shortens the polymer chain length and was used to convert the photon energy into mechanical work in a single polymer chain.[262]

As the knowledge of single-chain mechanics improves, the rational bottom-up design of polymer materials appears increasingly at hand. For example, Wu et al.[263] have produced hydrogels that are stiff but weak (brittle), soft but strong (highly stretchable) with low toughness, or strong and tough based on a common design principle. Namely, they connected folded polymer chains using physical cross-links and could tune the hydrogel's mechanical properties by varying the critical force needed to unfold one domain or break one cross-link.

Buried Polymer Interfaces. Consider a polymer that contains an isolated adsorbing moiety, say A, within a nonadsorbing chain B (Figure 2). The work of adhesion depends on the strength and surface density of the adhesive bonds between A and the surface. The density correlates with the bond strength; that is, stronger bonds are expected to produce a more abundant adsorption of A. On the other hand, the surface density also correlates with the mobility of A within the polymer, depending on the elasticity and dynamics of the nonadsorbing chain B. In this complex scenario, it is difficult to predict how many adhesive bonds will spontaneous appear because of adsorption or how many more will be formed by applying an external force and compressing the polymer against the surface. This general argument can be translated to the specific case of mussel adhesive proteins. These contain the Dopa moiety, showing a strong affinity for a variety of surfaces underwater.[46] However, mussel adhesive proteins adsorbed on a solid substrate do not always create adhesion at contact with another surface, even though they contain large amounts of Dopa.[264] The reason is that Dopa becomes strongly attached to the substrate during adsorption and there is no obvious free energy incentive for transferring Dopa onto another surface during contact. Even if there is an incentive, the mobility of Dopa in an adsorbed protein layer can be too low and the transfer time too long to produce significant adhesion.[241]

The previous example illustrates the challenge of the connecting molecular-scale processes to adhesion measurements. When the adhesive polymer has a heterogeneous composition, such as a protein or block copolymer, the adhesion

https://doi.org/10.1021/acs.macromol.1c01182
Macromolecules 2021, 54, 10617−10644

depends on the distribution of the different polymer residues at the interface with the adherend. Not only is this distribution difficult to predict, but the experimental study of the interface is challenging, because it is "buried" between two condensed materials.

Many techniques have been used to characterize polymer interfaces *in situ*, including ellipsometry, scanning probe microscopy (AFM, scanning tunneling microscopy (STM)), electron microscopy (scanning electron microscopy (SEM), transmission electron microscopy (TEM)), X-ray photoemission (XPS), secondary ion mass spectroscopy (SIMS), and various others. For a review, the reader can refer to refs 265 and 266. Only a few techniques, however, are able to assess the binding of specific residues at the interface between a polymer adhesive and an adherend. The main obstacle to common surface spectroscopies is that the materials at either side of the interface interact strongly with beams of electrons, ions, neutrons, and X-rays. This produces a background signal much stronger than the one coming from the interface, complicating the data analysis. Moreover, many techniques require placing the sample in vacuum or low-pressure gases to have a free path for the input probe and output signal to reach the sample and detector, respectively. In comparison, the interaction of optical photons with condensed materials is much weaker and allows studying transparent and reflective polymer−liquid, polymer−solid, and polymer−polymer interfaces.

A common approach to enhancing the surface sensitivity of optical spectroscopies is to place the sample in the evanescent wave created by total internal reflection at the interface between two transparent materials with different optical indices, such as water and high-optical index glass. Because the evanescent wave decays exponentially as a function of the distance from the interface, the measurements average the contributions of polymer residues that are at distances from the interface smaller than the decay length. For example, attenuated total reflection infrared spectroscopy (ATR-IR) has been used to study the displacement of water molecules and adsorption of Dopa residues at the interface between green mussel adhesive proteins and a TiO_2 substrate[267] and solvent uptake by a surface-grafted polymer brush.[268] Moreover, ATR-Raman was used to localize polystyrene−polycarbonate interfaces in a polymer stack, with a resolution of tens of nanometers.[269] The decay length of the evanescent wave, however, exceeds 100 nm and limits the resolution of ATR spectroscopies.[265,266] Another common approach to surface-sensitive optical spectroscopy is to place the sample in the electromagnetic field of a surface plasmon resonance at a metal surface. The resonance produces a nonradiative electromagnetic surface wave that propagates in a direction parallel to the metal surface and is very sensitive to any change of the boundary properties, such as variations of optical index due to molecule adsorption. Surface-enhanced fluorescence (SEF) and Raman spectroscopy (SERS) have been used to reveal the surface binding of specific polymer molecules to metal surfaces and the electrochemistry of adsorption and desorption as a function of the metal electrode potential, relevant to the long-term stability of polymer adhesives in corrosive environments.[270] SEF and SERS, however, not only are limited to the study of polymer−metal interfaces, but their sensitivity also depends on the morphology of the metal surface. Indeed, surface plasmon resonance is enhanced near the nanoscale asperities of roughened surfaces, nanofabricated tips, or metal nanoparticles at the interface with a polymer. Because of these specificities, SEF and SERS have found only limited applications in polymer adhesion.

Sum frequency generation (SFG) is a type of optical vibrational spectroscopy with unique capabilities for the characterization of solid−air, solid−liquid, and solid−solid interfaces. Excellent reviews on SFG studies on buried polymer interfaces can be found in refs 271−276. SFG is based on a nonlinear optical process in which two input laser beams with frequencies ω_1 and ω_2 mix in a medium and generate an output beam with frequency $\omega_1 + \omega_2$. The process requires a nonzero second-order dielectric susceptibility χ_{ijk}, which is a statistical average of the molecular hyper-polarizabilities α_{ijk} and depends on molecular order (the *ijk* indices indicate a third-rank tensor). The susceptibility χ_{ijk} is zero and SFG is forbidden in centrosymmetric materials, including most polymers and solids. Interfaces, however, break the inversion symmetry and can generate an SFG output signal. If either one or both frequencies ω_1 and ω_1 are scanned over surface resonances, SFG is resonantly enhanced, thus producing a spectrum characteristic of the surface. This method not only can differentiate chemical species according to their spectroscopic signature but also reveals the orientation of chemical species at the interface via beam polarization analysis and can dynamically resolve the changes in surface composition and structure induced by oxidation, chemical reactions, adsorption, and surface treatments such as exposure to solvents, plasma, solvent, and UV. For example, SFG was able to detect the alignment of aromatic rings on a polystyrene surface caused by mechanical rubbing (a method commonly used to align liquid crystals in display technology).[277] The composition and molecular order of interfaces between common polymer adhesives, such as epoxies and silicones, and glass, metals, oxides, and other polymers has been extensively studied in air[276] and can be directly related to adhesion strength by combining SFG with a JKR apparatus (Figure 3b).[278] SFG studies have focused less frequently on polymer−solid interfaces in liquids, where adhesion and friction critically depend on molecular layers of interstitial liquid, particularly in water.[278−280] The interest in "wet" polymer−solid interfaces, however, is rapidly growing due to recent advances in the understanding and biomimetic synthetic replication of biological adhesives (see the next section). Myers et al.[281] have related the diffusion of water molecules into epoxy/glass or epoxy/plastic interfaces to a decrease of adhesion. Chen, Wilkers, and co-workers have studied the surface binding of Dopa in mussel foot proteins.[282,283] Dhinojwala and co-workers have used SFG to correlate adhesion with the interfacial distribution of surface-bound water molecules and cross-interface molecular bounds for hydrophobic and hydrophilic surfaces, and glass and sapphire surfaces in contact with aggregate spider glue[284] and Dopa-based biomimetic adhesives.[285,286] Due to its unique surface sensitivity, SFG will likely increase in popularity among researchers working on novel polymer adhesives that contain specific surface-binding or cross-linking residues such as Dopa, particularly for applications in wet environments.

Wet Polymer Adhesives. Common polymers adhere poorly in moist conditions and underwater, particularly on strongly hydrophilic surfaces, such as metals and glass, and hydrated materials, such as clays, hydrogels, and biological tissues. In general, a condensed fluid like water interferes with the macroscopic adhesion of two materials, say 1 and 2, compared to a gas medium or vacuum. Indeed, while the work of adhesion is $W_{12} > 0$ in the latter case (eq 3), meaning that the

https://doi.org/10.1021/acs.macromol.1c01182
Macromolecules 2021, 54, 10617−10644

two materials always adhere to each other, the work of adhesion in a fluid 3 is given by[15]

$$W_{132} = W_{12} - W_{13} - W_{23} + W_{33} \quad (30)$$

The materials adhere to or are repelled by each other depending on the sign of W_{132}. On hydrophilic polar surfaces, W_{23} is comparable or larger than $W_{33} = 2\gamma_3$ (see eq 2), and therefore, the work of adhesion in water is reduced: $W_{123} < W_{12}$. For example, epoxy adheres strongly to aluminum in air or vacuum, with a work of adhesion W_{12} of the order of 100 mJ/m^2, but it is repelled by the metal in water.[2,257] To compensate for the effect of water, materials 1 and 2 should interact with each other more favorably than with water, so as to increase W_{12} as much as possible.

At the molecular level, water deeply affects physical interactions and therefore the ability of polymer segments to adhere to a surface or create cohesive cross-links.[15] First, the van der Waals attraction between two molecules is weaker in a condensed fluid than in vacuum. Second, electrostatic interactions of charges and dipoles depend on the reciprocal of the relative permittivity of the medium, which for water takes a high value $\epsilon_r \approx 80$. Moreover, in a strongly polar material such as water, charge interactions are screened by dissolved ions. Water also interferes with hydrogen bonding interactions, competing both as a hydrogen bond donor and acceptor, but it can promote the association between nonpolar functional groups and extended surfaces through the hydrophobic effect.[287,288] Finally, the aqueous environment obviously affects also the chemistry of adhesive bonds, e.g., by shifting the equilibria of hydrolysis and condensation reactions, or through environmental factors such as pH or the presence of reducing/oxidizing agents.

Tissue Adhesives. The research on "wet" polymer adhesives is fuelled by a strong demand coming from the medical field, particularly surgery, regenerative medicine, and tissue engineering.[13,289] For example, surgical sutures typically are made using needle and thread, or staples in time-sensitive interventions. Sutures not only produce tissue damage and inflammation but also are difficult or unfeasible at some surgical sites, such as the placenta or the retina. A less invasive and accurate surgical intervention could apply an adhesive locally, for instance with a syringe during endoscopy. Polymer coatings and "primers" could also be used to promote cell adhesion and growth on tissue scaffold materials, and integration of organ transplants and artificial implants in the human body. Moreover, hydrogels based on natural polymers such as gelatin, alginate, hyaluronic acid, dextran, chitosan, and known biocompatible materials such as PEG degrade naturally in the body without releasing toxic byproducts. "Smart" hydrogels that respond to physicochemical stimuli such as temperature, pH, enzymes, or electromagnetic fields are increasingly used to deliver drugs, nutrients, or cells at specific sites or to stimulate tissue morphogenesis and functions (e.g., via chemo-mechanical actuation).[290−292] Soft, transparent and responsive hydrogels are also used in optics, microfluidics, flexible electronics, and microrobotics, typically at contact with diverse materials such as glass, silicon, ceramics, metals, plastics, and elastomers.[12] When biocompatibility is not required, such as for bonding hydrogels with inorganic surfaces, surface functionalization with highly reactive silane groups is an effective strategy to achieve strong adhesion.[293]

All these applications require joining a polymer with another material in the presence of water. Human tissues are particularly challenging targets, as they typically have a water content exceeding 60%. A common strategy to increase both the adhesion and mechanical strength of polymer materials is to engineer strong water-compatible covalent bonds at the polymer interface and in the bulk (i.e., cross-links), as shown in Figure 2. The majority of polymer tissue adhesives approved or undergoing clinical trials for medical use are based on reactive groups that covalently bind to tissue functional groups. The reactive groups include cyanoacrylates, urethanes, *N*-hydroxysuccinimide (NHS) esters, aldehydes, catechol, isocyanates, and aryl azides.[13,289] These groups are either polymerized or grafted onto the main chain of a biocompatible polymer. Tissue functional groups include primary amines, carboxylic groups, and thiols of the surface proteins (e.g., in lysine, glutamic acid, and cysteine amino acids, respectively), with amines being the most widely targeted because of their abundance and variety of chemical reactions. One of the earliest demonstrations of this approach is fibrin glue, a medical adhesive approved for medical application and inspired by the biochemistry of blood clotting.[294] Fibrin is a fibrous protein that polymerizes in the presence of the enzyme thrombin, forming a weak polymer network. Thrombin also activates transglutaminase, an enzyme catalyzing amide bond formation between lysine and glutamine amino acids, thereby consolidating the fibrin network.

Biomimetic Adhesives. Finding an optimal balancing point for adhesion, strength, and toughness is crucial in many polymer applications and calls for a deeper understanding of how to harness the strength and kinetics of various types of molecular bonds (Figure 2) into macroscopic mechanical properties (Figure 7). To understand how these features originate from molecular bonds and interactions, natural materials and living organisms are increasingly viewed as a source of inspiration for biomimetic research.[234,295−300]

Hard natural materials such as bone, seashells, and wood have a hierarchical structure based on nanosized building blocks: collagen fibrils reinforced with hydroxyapatite crystals, calcium carbonate platelets, and cellulose fibrils, respectively. These blocks are connected by minor amounts of disordered, soft, and hydrated polymeric materials—an organic matrix comprising mainly proteins and polysaccharides.[258,301] This type of structure enables multiple mechanisms of deformation and energy dissipation that synergistically increase both strength and toughness above the levels provided by the single constituents. The toughness of bone, for example, is regulated by proteins of the organic matrix that show an abundance of anionic amino acids, notably phosphorylated serines. The protein osteopontin, named from Latin after its "bone-bridging" ability, is intrinsically disordered and binds to Ca^{2+} ions in solution and to calcium-containing minerals such as hydroxyapatite. It can dissipate large amounts of energy within the organic bone matrix by breaking the ion bridges formed by the association of phosphorylated protein segments and Ca^{2+} ions (Figure 2).[259,261,302] In the nacre of abalone seashells, the mineral platelets are connected by an organic matrix containing a highly modular protein named lustrin A.[258] Under a large tensile stress, lustrin A elongates by breaking partially folded portions of the protein sequence (Figure 2), thereby dissipating energy and enhancing the nacre fracture toughness.

In the past 15 years, the biomimetic development of wet adhesives has been energized by a series of studies on mussels of the genus *Mytilus* and *Perna* and on sandcastle worms (*Phragmatopoma californica*), exhibiting an impressive ability to attach to a wide variety of submerged surfaces using tough water-resistant proteinaceous secretions. These works have

https://doi.org/10.1021/acs.macromol.1c01182
Macromolecules 2021, 54, 10617−10644

highlighted the key role of the nonstandard aromatic amino acid 3,4-dihydroxy-L-phenylalanine (Dopa) (Figure 8), found in unusually large amounts in the adhesive secretions of both mussels and sandcastle worms. The catechol group in Dopa enables a rich and versatile chemistry for surface adhesion and tissue cohesion, which has been extensively discussed in several recent reviews (Figure 8).[46,300,303] The chemistry of Dopa overlaps with that of dopamine, a human neurotransmitter that polymerizes into poly(dopamine), melanin, and other compounds used in energy, environment, and medical applications.[304] In contrast with osteopontin, lustrin A, and the numerous other examples of cell-bound proteins (e.g., cadherins, biotin−streptavidin complex)[236] that express their adhesive function in a relatively closed and regulated environment, Dopa is secreted into an open and unpredictable environment. While reproducing specific protein structures and complex networks of interactions with synthetic materials is a daunting task, including Dopa in a synthetic polymer involves relatively simple chemical reactions and opens the exciting possibility of encoding nonspecific "all-purpose" adhesion mechanisms. This idea has had great appeal in material science and has led to a massive wave of research on Dopa-based polymers, recently covered in several reviews.[295−297,299,300]

A key feature in mussel and sandcastle worm adhesion is that Dopa can generate strong adhesion and tissue cohesion without necessarily creating covalent bonds. Indeed, Dopa can form many types of physical bonds, including hydrogen bonds, metal coordination complexes,[48,305,306] hydrophobic interactions, $\pi-\pi$ and cation$-\pi$[45] interactions (Figure 8) on a variety of surfaces, including hydrophilic glass, metals, metal oxides, plastics, and even antiadhesive Teflon coatings. Although weaker than covalent bonds, physical interactions are reversible and typically depend on the aqueous environment, providing a versatile molecular toolbox for engineering sacrificial bonds for tuning and actively controlling the mechanical properties of a polymer material. For instance, hydrogen bonds can be denatured by increasing temperature and decreasing pH, and metal coordination complexes change to higher coordination numbers with increasing pH, resulting in stronger protein binding.[46,301] Physical bonds that break and reform in a polymer network also introduce bond relaxation time and diffusivity as tuning parameters, in addition to bond strength. Thus, metal coordination bonds with the same thermodynamic equilibrium constant and different kinetic constants produce hydrogels with substantially different viscoelastic properties.[307]

The hydroquinone moiety of Dopa spontaneously oxidizes into quinone in seawater (pH > 7), and both mussels and sandcastle worms cosecrete catechol oxidase to regulate the redox state of Dopa amino acids.[46] Although quinone has a much lower surface affinity, primarily due to the lack of hydrogen-bonding capability, it can form covalent bonds with catechols, primary amines, and cysteines (Figure 8) that strengthen the adhesive material after surface deposition.[46,296,308] In the adhesive secretions of mussels and sandcastle worms, the curing process is completed by metal ions that diffuse from seawater and form complexes with catechols..[46]

Catechol has been incorporated into various polymer materials, particularly those already used for biomedical applications such as chitosan, PEG, hyaluronic acid, and alginate, producing materials with enhanced adhesion and interesting mechanical properties.[46,300,309] However, it is also becoming increasingly clear that the inclusion of Dopa does not guarantee the adhesive performance of a polymer material. Several key aspects of mussel adhesion, listed below, are still be to be clarified for improving biomimetic adhesives.

1. A major obstacle is controlling the oxidation of catechol into quinone.[310] Mussels rely on various molecular and biological mechanisms, including a redox synergy between catechol and cysteine amino acids, as well as morphological features of the adhesive mussel foot, that have not yet been reproduced in synthetic material.[298] Moreover, in both mussels and sandcastle worms adhesive proteins the hydrophobic amino acid glycine is mostly located near Dopa, suggesting that glycine may protect Dopa from oxidization.[311] The introduction of borate, which can form hydrogen bonds with both hydroxyl groups of Dopa, effectively protects it from oxidation without decreasing its adhesive properties.[312]
2. Mussels are known to secrete their adhesive proteins in a time-regulated sequence, starting from "vanguard" proteins with a high Dopa content.[313] While vanguard proteins displace water molecules from the substrate and establish adhesive surface−protein bonds, the role of the other proteins is to build the strong and tough connective tissue of the mussel adhesive and create a hard protective coating at the interface with seawater through an elaborate network of protein−protein interactions.[298] Synthetic adhesives, on the other hand, encode multiple functions in a single polymer structure, without matching the complexity and efficiency of protein adhesives.
3. The abundance and proximity of aromatic Dopa and cationic lysine in mussel adhesive proteins enables a synergy between these amino acids that has rarely been included in mussel-inspired adhesives.[314] Namely, lysine evicts hydrated ions from polar negatively charged surfaces such as mica, facilitating the adsorption of catechol.
4. Mussels' and sandcastle worms' adhesion hinges on a delicate balance between adhesive surface−protein bonds and cohesive protein cross-links, both involving Dopa.[315] The abundance of cationic lysine and arginine amino acids in mussel foot proteins suggests the formation of strong cohesive cation$-\pi$ bonds.[45,314] Yet, the type, strength, and distributions of cohesive bonds within an adhesive layer of Dopa proteins have not yet been fully characterized or related to the adhesion generated at contact with another surface.
5. There is growing evidence that aromatic amino acids such as tyrosine and phenylalanine can replicate some if not most of the adhesive and cross-linking features of Dopa. For example, recombinant green mussel adhesive proteins[316] and synthetic polypeptides[45,47] in which Dopa was replaced with tyrosine or phenylalanine showed adhesion comparable to those obtained with the Dopa-containing versions.
6. In addition to hydroxylation of tyrosine into Dopa, phosphorylation of serine amino acids by addition of the anionic phosphate group is common in both mussels and sandcastle worms and enables surface-binding and cross-linking via Ca^{2+} ion bridges.[261,302] Moreover, phosphorylation engages the numerous cationic residues (lysine and arginine) in electrostatic interactions.[46]
7. The proteins of the sandcastle worm adhesive are either phosphorylated and anionic, or cationic. Electrostatic

https://doi.org/10.1021/acs.macromol.1c01182
Macromolecules 2021, 54, 10617−10644

interactions between these two protein groups drive complex coacervation, i.e., the spontaneous separation into a protein-rich fluid phase and a protein-deficient aqueous phase.[317,318] Self-coacervation was also observed for cationic mussel adhesive proteins.[319−321] In the absence of a cationic counterpart, it has been proposed that self-coacervation is driven by cation−π and $\pi-\pi$ interaction within the same protein as well as electrostatic interactions between oppositely charged amino acids. Complex coacervation is a promising strategy to increase the efficiency of polymer adhesives as it densifies them and enhances their spreading and delivery on the surface, owing to the low interface energy with the surrounding aqueous phase (eqs 3 and 4). Moreover, it has been shown that complex coacervation of recombinant cationic mussel adhesive proteins with a polycation such as HA produces an increase of adhesive strength compared to the single components.[322,323]

Biomimetics beyond Dopa. Far from being a prerogative of mussels and sandcastle worms, underwater adhesion underlies a dazzling variety of biological purposes at different scales of size and complexity[324] and is typically provided by polymeric materials such as DNA, proteins, and polysaccharides.[325] In the past few years, the search for new bioadhesives has expanded at an unprecedented rate. The contributions on mussels and sandcastle worms have helped establish a transdisciplinary framework for translating adhesion-related concepts, materials, and methods from biology to chemistry, nanoscience, and material science.[324] For example, material scientists have promptly adopted rapid RNA sequencing as a tool for identifying putative adhesive proteins from the footprint left on the surface by an adhesive organism.[324,326]

For most multicellular aquatic organisms, adhesion is a key function not only for surface attachment but also for prey capture, protection, defense, mating, locomotion, parasitism, and the building of dwellings.[324] One of the most highly conserved defense strategies against microbial infection across the animal kingdom is the secretion of a slimy hydrogel known as mucus.[327] Its main purpose is to trap and immobilize pathogens, such as viruses and microbes, and dust particles. These are transported and eventually cleared from the interface within the mucus layer, e.g., by continuous mucus secretion or motion of surface cilia in human airways. Inspired by the sticky mucous slime of the *Arion subfuscus* slug, Celiz and co-workers[9] have produced an effective hydrogel tissue adhesive that combines two biocompatible polymers. A "bridging" polymer containing primary amines (e.g., chitosan) was inserted at the interface between an alginate-acrylate hydrogel and the tissue. Although the hydrogel does not adsorb to the tissue, both the tissue and the hydrogel bear carboxylic acids that bind to the amines. Therefore, the bridging polymer provides tissue adhesion and transfers mechanical stresses to the hydrogel, where they can be effectively dissipated and produce a very large toughness. Recently, Steinbauer et al.[256] studied a short amino acid sequence containing phosphoserine that is involved in various protein adsorption processes at the interface with mineralized tissue of the human body. Notably, the sequence is found in the ostepontin and statherin proteins that bind to hydroxyapatite crystals of the tooth enamel and therefore is a good candidate for developing wet polymer adhesives that target human bone and teeth.

It is likely that the study of adhesive materials secreted by aquatic organisms will provide new insights on how to generate adhesion with polymers in water. Microscopic organisms such as bacteria, fungi, and archaea are able to attach to wet surfaces by secreting multifunctional adhesive biofilms.[325] Oral cavities, for example, are caused by bacteria that bind and thrive on wet tooth surfaces despite being continuously exposed to mechanical stresses. Yet, to date only a few studies have tried to replicate the molecular basis of bacterial adhesion into synthetic polymer adhesives.[328,329] Many reviews on bioadhesives produced by marine invertebrates other than mussels, barnacles, and sandcastle worms have appeared recently,[324,330] highlighting a variety of adhesion strategies and providing new ideas for the development of biomimetic polymers beyond the inclusion of Dopa. In particular, echinoderms such as sea stars[331] and sea urchins[332] secrete Dopa-free proteins to adhere to and detach from submerged surfaces during locomotion. The secretion contains many distinct proteins, some of which are left on the surface after detachment, suggesting a direct involvement in adhesion. While identifying the role of each protein is a complex experimental task, the study of sea urchins and sea stars has already highlighted the importance of non-Dopa amino acid modifications, particularly a high degree of glycosylation and phosphorylation. It would not be surprising if the ongoing intense research effort on the adhesion of marine invertebrates would soon produce new breakthroughs.

CONCLUSIONS

In our overview of polymer adhesion, we have covered recent advances in the areas of the theory and simulation of adhesion phenomena, the experimental measurement of molecularly resolved interfacial forces and structures, and the development of biologically inspired underwater adhesives. We close this Perspective by summarizing our views on the future challenges in these areas:

- Improving our understanding of adhesive bonding, starting from the molecular level, but remembering that it is the macro-scale that matters.
- Integrating seamlessly the computational approaches to adhesion problems, from electronic structure calculations of bonding at organic−inorganic interfaces to continuum approaches to contact mechanics and fluid flow.
- Developing the theoretical tools that are necessary to deal with extreme nonequilibrium phenomena, such as polymer fracture and debonding.
- Promoting the sharing, integration, and comparison of experimental, theoretical, and computational data on adhesive interfaces.
- Directly measuring the nanoscale deformations and mechanical forces of polymer films, monolayers, and single molecules, and resolving the distribution, orientation, and interactions of adhesive molecular groups (e.g., Dopa) at a polymer interface. The role of polymer interphases has been stressed in the field of nanocomposites,[173,333,334] but it has not yet been explored systematically for polymer adhesion and friction.
- Expanding the database of model parameters such as single-chain elasticity, dissociation−association dynamics, unfolding energy of protein domains, and collective mechanical response of dense polymer monolayers (e.g., brushes).

https://doi.org/10.1021/acs.macromol.1c01182
Macromolecules 2021, 54, 10617−10644

- Enabling the rational bottom-up design of polymers with specific adhesive and mechanical properties from the knowledge of their molecular properties.
- Controlling adhesion and mechanical forces with non-mechanical stimuli such as ions and electric fields for polyelectrolytes, and UV-irradiation for azobenzene-containing polymers, to achieve an active control of the adhesive properties (e.g., adhesion "on demand").
- Building a rich and versatile molecular toolbox of molecular structures and interactions to engineer the adhesion and mechanical response of polymers and hydrogels. Precision polymer synthesis, which can place functional groups at better controlled densities and locations, may play an increasingly important role in further understanding adhesion phenomena.
- Searching new mechanisms of underwater adhesion among the myriad examples provided by living organisms.

AUTHOR INFORMATION

Corresponding Authors

Guido Raos − *Department of Chemistry, Materials and Chemical Engineering "G. Natta", Politecnico di Milano, I-20131 Milano, Italy;* orcid.org/0000-0001-7011-4036; Email: guido.raos@polimi.it

Bruno Zappone − *Consiglio Nazionale delle Ricerche - Istituto di Nanotecnologia (CNR-Nanotec), 87036 Rende (CS), Italy;* orcid.org/0000-0003-3002-4022; Email: bruno.zappone@cnr.it

Complete contact information is available at: https://pubs.acs.org/10.1021/acs.macromol.1c01182

Notes

The authors declare no competing financial interest.

Biographies

Guido Raos obtained a degree in chemistry from the Università degli Studi di Milano and a Ph.D. in theoretical chemistry from the University of Bristol. Since 1993 he has been at the Politecnico di Milano, where he is now full professor of chemistry. He is a member of IUPAC's Polymer Division.

Bruno Zappone obtained a degree in physics at the University of Calabria and a Ph.D. in soft matter physics at the University of Bordeaux. He worked as a postdoc researcher at the University of California, Santa Barbara, in Prof. J. Israelachvili's group and at the Centre de Recherche "Paul Pascal" in Bordeaux. He currently is a researcher at CNR-Nanotec, where he studies the nanoscale physics of soft and biological materials and interfaces.

ACKNOWLEDGMENTS

G.R. was introduced to polymer science by Giuseppe Allegra in 1993 and has enjoyed the scientific collaboration and personal friendship with him for many years since then. G.R. also thanks Stefano Valdo Meille for his kind encouragement and Ugo Tartaglino, Andrey Milchev, and Vahktang Rostiashvili for discussions. B.Z. thanks Pasquale Pagliusi and Marco Castriota of the University of Calabria for useful discussions.

DEDICATION

#This work is dedicated to Giuseppe Allegra (1933−2019). Giuseppe Allegra obtained a degree in chemical engineering from the Politecnico di Milano (1958). His early work with Giulio Natta and Paolo Corradini was on crystallographic problems, including the elucidation of the crystal structure of organometallic compounds, polymerization catalysts, and polymers. He contributed also to the theory of diffraction by partially disordered systems and to the direct methods for the solution of crystal structures. Soon he became interested in the calculation of the conformational properties of polymers, and from there he progressed to attack problems in the statistical physics of polymers. This included the theory of rubber elasticity, polymer crystallization, the structural and dynamical properties of polymers in solution, and rubber reinforcement. Most of his career was spent at the Politecnico di Milano, but for a period he was professor at the University of Trieste and a visitor at the Brooklyn Polytechnic and at IBM in San Jose. He was a member of the Accademia dei Lincei. He was also president of the Italian crystallographic association and the first president of the Italian macromolecular association.

REFERENCES

(1) Staudinger, H. Über polymerisation. *Ber. Dtsch. Chem. Ges. B* **1920**, *53*, 1073−1085.

(2) Pocius, A. V. *Adhesion and Adhesives Technology*, 3rd ed.; Hanser Verlag: Munich, 2012.

(3) Baldan, A. Adhesively-bonded joints and repairs in metallic alloys, polymers and composite materials: Adhesives, adhesion theories and surface pretreatment. *J. Mater. Sci.* **2004**, *39*, 1−49.

(4) Flory, P. J. *Principles of polymer chemistry*; Cornell University Press, 1953.

(5) de Gennes, P.-G. *Scaling concepts in polymer physics*; Cornell University Press, 1979.
(6) Doi, M.; Edwards, S. F. *The theory of polymer dynamics*; Oxford University Press, 1988.
(7) Grosberg, A. Y.; Khokhlov, A. R. *Statistical physics of macromolecules*; AIP Press, 1994.
(8) Rubinstein, M.; Colby, R. H. *Polymer physics*; Oxford university Press: Oxford, 2003.
(9) Li, J.; Celiz, A. D.; Yang, J.; Yang, Q.; Wamala, I.; Whyte, W.; Seo, B. R.; Vasilyev, N. V.; Vlassak, J. J.; Suo, Z.; Mooney, D. J. Tough adhesives for diverse wet surfaces. *Science* **2017**, *357*, 378−381.
(10) Bovone, G.; Dudaryeva, O. Y.; Marco-Dufort, B.; Tibbitt, M. W. Engineering Hydrogel Adhesion for Biomedical Applications via Chemical Design of the Junction. *ACS Biomater. Sci. Eng.* **2021**, *7*, 4048.
(11) Zhang, Y. S.; Khademhosseini, A. Advances in engineering hydrogels. *Science* **2017**, *356*, No. eaaf3627.
(12) Yang, J.; Bai, R.; Chen, B.; Suo, Z. Hydrogel Adhesion: A Supramolecular Synergy of Chemistry, Topology, and Mechanics. *Adv. Funct. Mater.* **2020**, *30*, 1901693.
(13) Nam, S.; Mooney, D. Polymeric Tissue Adhesives. *Chem. Rev.* **2021**, *121*, 11336.
(14) de Gennes, P.-G.; Brochard-Wyart, F.; Quéré, D. *Capillarity and Wetting Phenomena*; Springer: New York, NY, 2004; p 291, DOI: 10.1007/978-0-387-21656-0.
(15) Israelachvili, J. N. *Intermolecular and surface forces*, 3rd ed.; Academic Press, 2011.
(16) Elliott, J. A. Gibbsian Surface Thermodynamics. *J. Phys. Chem. B* **2020**, *124*, 10859−10878.
(17) Fetters, L. J.; Lohse, D. J.; Richter, D.; Witten, T. A.; Zirkel, A. Connection between Polymer Molecular Weight, Density, Chain Dimensions, and Melt Viscoelastic Properties. *Macromolecules* **1994**, *27*, 4639−4647.
(18) Kawana, S.; Jones, R. Effect of physical ageing in thin glassy polymer films. *Eur. Phys. J. E: Soft Matter Biol. Phys.* **2003**, *10*, 223−230.
(19) Ediger, M. D.; Forrest, J. a. Dynamics near Free Surfaces and the Glass Transition in Thin Polymer Films: A View to the Future. *Macromolecules* **2014**, *47*, 471−478.
(20) Schweizer, K. S.; Simmons, D. S. Progress towards a phenomenological picture and theoretical understanding of glassy dynamics and vitrification near interfaces and under nanoconfinement. *J. Chem. Phys.* **2019**, *151*, 240901.
(21) Dee, G. T.; Sauer, B. B. The surface tension of polymer liquids. *Adv. Phys.* **1998**, *47*, 161−205.
(22) Griffith, A. A. VI. The phenomena of rupture and flow in solids. *Philosophical Transactions of the Royal Society of London. Series A, Containing Papers of a Mathematical or Physical Character* **1921**, *221*, 163.
(23) Landau, L. D.; Pitaevskii, L. P.; Kosevich, A. M.; Lifshitz, E. M. *Course of theoretical physics: theory of elasticity*, 3rd ed.; Butterworth-Heinemann, 1984.
(24) Guimarães, C. F.; Gasperini, L.; Marques, A. P.; Reis, R. L. The stiffness of living tissues and its implications for tissue engineering. *Nature Reviews Materials* **2020**, *5*, 351−370.
(25) Irajizad, P.; Al-Bayati, A.; Eslami, B.; Shafquat, T.; Nazari, M.; Jafari, P.; Kashyap, V.; Masoudi, A.; Araya, D.; Ghasemi, H. Stress-localized durable icephobic surfaces. *Mater. Horiz.* **2019**, *6*, 758−766.
(26) Chaudhury, M. K.; Kim, K. H. Shear-induced adhesive failure of a rigid slab in contact with a thin confined film. *Eur. Phys. J. E: Soft Matter Biol. Phys.* **2007**, *23*, 175−183.
(27) Shull, K. R. Contact mechanics and the adhesion of soft solids. *Mater. Sci. Eng., R* **2002**, *36*, 1−45.
(28) Persson, B. N. J.; Albohr, O.; Tartaglino, U.; Volokitin, a. I.; Tosatti, E. On the nature of surface roughness with application to contact mechanics, sealing, rubber friction and adhesion. *J. Phys.: Condens. Matter* **2005**, *17*, R1−R62.
(29) Creton, C.; Ciccotti, M. Fracture and adhesion of soft materials: a review. *Rep. Prog. Phys.* **2016**, *79*, 046601.
(30) Johnson, K. L.; Kendall, K.; Roberts, A. D. Surface energy and the contact of elastic solids. *Proceedings of the Royal Society of London. A. Mathematical and Physical Sciences* **1971**, *324*, 301−313.
(31) Kendall, K. The adhesion and surface energy of elastic solids. *J. Phys. D: Appl. Phys.* **1971**, *4*, 1186−1195.
(32) Barthel, E. Adhesive elastic contacts: JKR and more. *J. Phys. D: Appl. Phys.* **2008**, *41*, 163001.
(33) Chaudhury, M. K.; Whitesides, G. M. Direct Measurement of Interfacial Interactions between Semispherical Lenses and Flat Sheets of Poly(dimethylsiloxane) and Their Chemical Derivatives. *Langmuir* **1991**, *7*, 1013−1025.
(34) Silberzan, P.; Perutz, S.; Kramer, E. J.; Chaudhury, M. K. Study of the Self-Adhesion Hysteresis of a Siloxane Elastomer Using the JKR Method. *Langmuir* **1994**, *10*, 2466−2470.
(35) Creton, C.; Brown, H. R.; Shull, K. R. Molecular Weight Effects in Chain Pullout. *Macromolecules* **1994**, *27*, 3174−3183.
(36) Deruelle, M.; Leger, L.; Tirrell, M. Adhesion at the Solid-Elastomer Interface: Influence of the Interfacial Chains. *Macromolecules* **1995**, *28*, 7419−7428.
(37) Tirrell, M. Measurement of Interfacial Energy at Solid Polymer Surfaces. *Langmuir* **1996**, *12*, 4548−4551.
(38) Gent, A.; Schultz, J. Effect of wetting liquids on the strength of adhesion of viscoelastic material. *J. Adhes.* **1972**, *3*, 281−294.
(39) Gent, A. N. Adhesion and strength of viscoelastic solids. Is there a relationship between adhesion and bulk properties? *Langmuir* **1996**, *12*, 4492−4495.
(40) Doi, M. *Soft matter physics*; Oxford University Press, 2013.
(41) Gent, A. N. In *Engineering with rubber*, 3rd ed.; Gent, A. N., Ed.; Hanser Publications, 2012.
(42) Phan-Thien, N. *Understanding Viscoelasticity*; Graduate Texts in Physics; Springer: Berlin, 2013; DOI: 10.1007/978-3-642-32958-6.
(43) Kim, J.; Zhang, G.; Shi, M.; Suo, Z. Fracture, fatigue, and friction of polymers in which entanglements greatly outnumber cross-links. *Science* **2021**, *374*, 212−216.
(44) Ritchie, R. O. The conflicts between strength and toughness. *Nat. Mater.* **2011**, *10*, 817−822.
(45) Gebbie, M. A.; Wei, W.; Schrader, A. M.; Cristiani, T. R.; Dobbs, H. A.; Idso, M.; Chmelka, B. F.; Waite, J. H.; Israelachvili, J. N. Tuning underwater adhesion with cation-p interactions. *Nat. Chem.* **2017**, *9*, 473−479.
(46) Hofman, A. H.; van Hees, I. A.; Yang, J.; Kamperman, M. Bioinspired Underwater Adhesives by Using the Supramolecular Toolbox. *Adv. Mater.* **2018**, *30*, 1704640.
(47) Deepankumar, K.; Lim, C.; Polte, I.; Zappone, B.; Labate, C.; De Santo, M. P.; Mohanram, H.; Palaniappan, A.; Hwang, D. S.; Miserez, A. Supramolecular β-Sheet Suckerin−Based Underwater Adhesives. *Adv. Funct. Mater.* **2020**, *30*, 1907534.
(48) Khare, E.; Holten-Andersen, N.; Buehler, M. J. Transition-metal coordinate bonds for bioinspired macromolecules with tunable mechanical properties. *Nature Reviews Materials* **2021**, *6*, 421.
(49) Lake, G. J.; Thomas, A. G. The strength of highly elastic materials. *Proceedings of the Royal Society of London. Series A. Mathematical and Physical Sciences* **1967**, *300*, 108−119.
(50) Gong, J. P.; Katsuyama, Y.; Kurokawa, T.; Osada, Y. Double-Network Hydrogels with Extremely High Mechanical Strength. *Adv. Mater.* **2003**, *15*, 1155−1158.
(51) Gong, J. P. Why are double network hydrogels so tough? *Soft Matter* **2010**, *6*, 2583.
(52) Creton, C. 50th Anniversary Perspective: Networks and Gels: Soft but Dynamic and Tough. *Macromolecules* **2017**, *50*, 8297−8316.
(53) Brown, H. R. The adhesion of polymers: Relations between properties of polymer chains and interface toughness. *J. Adhes.* **2006**, *82*, 1013−1032.
(54) Binder, K.; Horbach, J.; Vink, R.; De Virgiliis, A. Confinement effects on phase behavior of soft matter systems. *Soft Matter* **2008**, *4*, 1555.
(55) Baschnagel, J.; Varnik, F. Computer simulations of supercooled polymer melts in the bulk and in confined geometry. *J. Phys.: Condens. Matter* **2005**, *17*, R851.

https://doi.org/10.1021/acs.macromol.1c01182
Macromolecules 2021, 54, 10617−10644

(56) Zaccone, A.; Noirez, L. Universal G L − 3 Law for the Low-Frequency Shear Modulus of Confined Liquids. *J. Phys. Chem. Lett.* **2021**, *12*, 650−657.
(57) Schmid, F. Self-consistent-field theories for complex fluids. *J. Phys.: Condens. Matter* **1998**, *10*, 8105−8138.
(58) Wu, J.; Li, Z. Density-Functional Theory for Complex Fluids. *Annu. Rev. Phys. Chem.* **2007**, *58*, 85−112.
(59) Muthukumar, M. 50th Anniversary Perspective: A Perspective on Polyelectrolyte Solutions. *Macromolecules* **2017**, *50*, 9528−9560.
(60) La Mantia, F.; Morreale, M.; Botta, L.; Mistretta, M.; Ceraulo, M.; Scaffaro, R. Degradation of polymer blends: A brief review. *Polym. Degrad. Stab.* **2017**, *145*, 79−92.
(61) Allegra, G.; Meille, S. V. The bundle theory for polymer crystallisation. *Phys. Chem. Chem. Phys.* **1999**, *1*, 5179−5188.
(62) Allegra, G.; Famulari, A. Chain statistics in polyethylene crystallization. *Polymer* **2009**, *50*, 1819−1829.
(63) Muthukumar, M. In *Progress in Understanding of Polymer Crystallization*; Reiter, G., Strobl, G. R., Eds.; Lecture Notes in Physics; Springer: Berlin, 2007; Vol. *714*; pp 1−18, DOI: 10.1007/3-540-47307-6_1.
(64) Lee, S.; Rutledge, G. C. Plastic Deformation of Semicrystalline Polyethylene by Molecular Simulation. *Macromolecules* **2011**, *44*, 3096−3108.
(65) Spyriouni, T.; Tzoumanekas, C.; Theodorou, D.; Müller-Plathe, F.; Milano, G. Coarse-Grained and Reverse-Mapped United-Atom Simulations of Long-Chain Atactic Polystyrene Melts: Structure, Thermodynamic Properties, Chain Conformation, and Entanglements. *Macromolecules* **2007**, *40*, 3876−3885.
(66) De Nicola, A.; Kawakatsu, T.; Milano, G. Generation of Well-Relaxed All-Atom Models of Large Molecular Weight Polymer Melts: A Hybrid Particle-Continuum Approach Based on Particle-Field Molecular Dynamics Simulations. *J. Chem. Theory Comput.* **2014**, *10*, 5651−5667.
(67) Theodorou, D. N.; Vogiatzis, G. G.; Kritikos, G. Self-consistent-field study of adsorption and desorption kinetics of polyethylene melts on graphite and comparison with atomistic simulations. *Macromolecules* **2014**, *47*, 6964−6981.
(68) Li, C.; Strachan, A. Molecular scale simulations on thermoset polymers: A review. *J. Polym. Sci., Part B: Polym. Phys.* **2015**, *53*, 103−122.
(69) David, A.; Tartaglino, U.; Raos, G. Towards realistic simulations of polymer networks: tuning vulcanisation and mechanical properties. *Phys. Chem. Chem. Phys.* **2021**, *23*, 3496−3510.
(70) David, A.; Tartaglino, U.; Casalegno, M.; Raos, G. Fracture in Silica/Butadiene Rubber: A Molecular Dynamics View of Design−Property Relationships. *ACS Polymers Au* **2021**, 1c00023.
(71) Allegra, G.; Raos, G.; Manassero, C. Polymer-mediated adhesion: A statistical approach. *J. Chem. Phys.* **2003**, *119*, 9295.
(72) Deam, R.; Edwards, S. F. The theory of rubber elasticity. *Philosophical Transactions of the Royal Society of London. Series A, Mathematical and Physical Sciences* **1976**, *280*, 317−353.
(73) Gay, C.; Leibler, L. On Stickiness. *Phys. Today* **1999**, *52*, 48−52.
(74) Zosel, A. The effect of fibrilation on the tack of pressure sensitive adhesives. *Int. J. Adhes. Adhes.* **1998**, *18*, 265−271.
(75) Lakrout, H.; Sergot, P.; Creton, C. Direct observation of cavitation and fibrillation in a probe tack experiment on model acrylic pressure-sensitive-adhesives. *J. Adhes.* **1999**, *69*, 307−359.
(76) Yamaguchi, T.; Morita, H.; Doi, M. Modeling on debonding dynamics of pressure-sensitive adhesives. *Eur. Phys. J. E: Soft Matter Biol. Phys.* **2006**, *20*, 7−17.
(77) Yamaguchi, T.; Doi, M. Debonding dynamics of pressure-sensitive adhesives: 3D block model. *Eur. Phys. J. E: Soft Matter Biol. Phys.* **2006**, *21*, 331−339.
(78) Huang, H.; Dasgupta, A.; Singh, N. Predictive mechanistic model for single-layered pressure-sensitive adhesive (PSA) joints. *Eur. Phys. J. E: Soft Matter Biol. Phys.* **2020**, *43*, 59.
(79) Yamaguchi, T.; Creton, C.; Doi, M. Simple model on debonding of soft adhesives. *Soft Matter* **2018**, *14*, 6206−6213.
(80) Kauzmann, W.; Eyring, H. The Viscous Flow of Large Molecules. *J. Am. Chem. Soc.* **1940**, *62*, 3113−3125.
(81) Mark, H. Natural and artificial rubber: The elasticity of long-chain molecules. *Nature* **1938**, *141*, 670−672.
(82) Makarov, D. E. Perspective: Mechanochemistry of biological and synthetic molecules. *J. Chem. Phys.* **2016**, *144*, 030901.
(83) Bell, G. I. Models for the specific adhesion of cells to cells. *Science* **1978**, *200*, 618−627.
(84) Evans, E.; Ritchie, K. Dynamic strength of molecular adhesion bonds. *Biophys. J.* **1997**, *72*, 1541−1555.
(85) Beyer, M. K.; Clausen-Schaumann, H. Mechanochemistry: The Mechanical Activation of Covalent Bonds. *Chem. Rev.* **2005**, *105*, 2921−2948.
(86) Huang, Z.; Boulatov, R. Chemomechanics: chemical kinetics for multiscale phenomena. *Chem. Soc. Rev.* **2011**, *40*, 2359.
(87) Ribas-Arino, J.; Marx, D. Covalent mechanochemistry: Theoretical concepts and computational tools with applications to molecular nanomechanics. *Chem. Rev.* **2012**, *112*, 5412−5487.
(88) Boswell, B. R.; Mansson, C. M. F.; Cox, J. M.; Jin, Z.; Romaniuk, J. A. H.; Lindquist, K. P.; Cegelski, L.; Xia, Y.; Lopez, S. A.; Burns, N. Z. Mechanochemical synthesis of an elusive fluorinated polyacetylene. *Nat. Chem.* **2021**, *13*, 41−46.
(89) De Bo, G. Polymer Mechanochemistry and the Emergence of the Mechanophore Concept. *Macromolecules* **2020**, *53*, 7615−7617.
(90) Bao, Y.; Luo, Z.; Cui, S. Environment-dependent single-chain mechanics of synthetic polymers and biomacromolecules by atomic force microscopy-based single-molecule force spectroscopy and the implications for advanced polymer materials. *Chem. Soc. Rev.* **2020**, *49*, 2799−2827.
(91) Ducrot, E.; Chen, Y.; Bulters, M.; Sijbesma, R. P.; Creton, C. Toughening Elastomers with Sacrificial Bonds and Watching Them Break. *Science* **2014**, *344*, 186−189.
(92) Radiom, M.; Kong, P.; Maroni, P.; Schäfer, M.; Kilbinger, A. F.; Borkovec, M. Mechanically induced cis-to-trans isomerization of carbon-carbon double bonds using atomic force microscopy. *Phys. Chem. Chem. Phys.* **2016**, *18*, 31202−31210.
(93) Huang, W.; Zhu, Z.; Wen, J.; Wang, X.; Qin, M.; Cao, Y.; Ma, H.; Wang, W. Single Molecule Study of Force-Induced Rotation of Carbon-Carbon Double Bonds in Polymers. *ACS Nano* **2017**, *11*, 194−203.
(94) Allegra, G.; Bruzzone, M. Effect of entropy of melting on strain-induced crystallization. *Macromolecules* **1983**, *16*, 1167−1170.
(95) Odell, J. A.; Muller, A. J.; Narh, K. A.; Keller, A. Degradation of polymer solutions in extensional flows. *Macromolecules* **1990**, *23*, 3092−3103.
(96) Huang, Q.; Hassager, O. Polymer liquids fracture like solids. *Soft Matter* **2017**, *13*, 3470−3474.
(97) Wagner, M. H.; Narimissa, E.; Huang, Q. Scaling relations for brittle fracture of entangled polystyrene melts and solutions in elongational flow. *J. Rheol.* **2021**, *65*, 311−324.
(98) Danielsen, S. P. O.; et al. Molecular Characterization of Polymer Networks. *Chem. Rev.* **2021**, *121*, 5042−5092.
(99) Zhang, W.; Zhang, X. Single molecule mechanochemistry of macromolecules. *Prog. Polym. Sci.* **2003**, *28*, 1271−1295.
(100) Wang, S.; Panyukov, S.; Rubinstein, M.; Craig, S. L. Quantitative Adjustment to the Molecular Energy Parameter in the Lake-Thomas Theory of Polymer Fracture Energy. *Macromolecules* **2019**, *52*, 2772−2777.
(101) Rubinstein, M.; Panyukov, S. Elasticity of polymer networks. *Macromolecules* **2002**, *35*, 6670−6686.
(102) Persson, B. N. J.; Albohr, O.; Heinrich, G.; Ueba, H. Crack propagation in rubber-like materials. *J. Phys.: Condens. Matter* **2005**, *17*, R1071−R1142.
(103) Slootman, J.; Waltz, V.; Yeh, C. J.; Baumann, C.; Göstl, R.; Comtet, J.; Creton, C. Quantifying Rate- and Temperature-Dependent Molecular Damage in Elastomer Fracture. *Phys. Rev. X* **2020**, *10*, 041045.
(104) Chaudhury, M. K. Rate-Dependent Fracture at Adhesive Interface. *J. Phys. Chem. B* **1999**, *103*, 6562−6566.

https://doi.org/10.1021/acs.macromol.1c01182
Macromolecules 2021, 54, 10617−10644

(105) Ghatak, A.; Vorvolakos, K.; She, H.; Malotky, D. L.; Chaudhury, M. K. Interfacial Rate Processes in Adhesion and Friction. *J. Phys. Chem. B* **2000**, *104*, 4018−4030.
(106) Schallamach, A. A. Theory of Dynamic Rubber Friction. *Rubber Chem. Technol.* **1966**, *39*, 320−327.
(107) Kramers, H. Brownian motion in a field of force and the diffusion model of chemical reactions. *Physica* **1940**, *7*, 284−304.
(108) Hänggi, P.; Talkner, P.; Borkovec, M. Reaction-rate theory: fifty years after Kramers. *Rev. Mod. Phys.* **1990**, *62*, 251−341.
(109) Gupta, V. K. Stochastic simulation of single-molecule pulling experiments. *Eur. Phys. J. E: Soft Matter Biol. Phys.* **2014**, *37*, 99.
(110) Allegra, G. Role of internal viscosity in polymer viscoelasticity. *J. Chem. Phys.* **1974**, *61*, 4910−4920.
(111) Allegra, G.; Ganazzoli, F. *Advances in Chemical Physics* **2007**, *75*, 265−348.
(112) Arbe, A.; Monkenbusch, M.; Stellbrink, J.; Richter, D.; Farago, B.; Almdal, K.; Faust, R. Origin of Internal Viscosity Effects in Flexible Polymers: A Comparative Neutron Spin-Echo and Light Scattering Study on Poly(dimethylsiloxane) and Polyisobutylene. *Macromolecules* **2001**, *34*, 1281−1290.
(113) Langer, J. S. Statistical theory of the decay of metastable states. *Ann. Phys.* **1969**, *54*, 258−275.
(114) Sain, A.; Dias, C. L.; Grant, M. Rupture of an extended object: A many-body Kramers calculation. *Phys. Rev. E* **2006**, *74*, 046111.
(115) Ghosh, A.; Dimitrov, D. I.; Rostiashvili, V. G.; Milchev, A.; Vilgis, T. A. Thermal breakage and self-healing of a polymer chain under tensile stress. *J. Chem. Phys.* **2010**, *132*, 204902.
(116) Voter, A. F. *Radiation Effects in Solids*; Springer: Dordrecht, 2007; pp 1−23, DOI: 10.1007/978-1-4020-5295-8_1.
(117) Paturej, J.; Milchev, A.; Rostiashvili, V. G.; Vilgis, T. A. Polymer chain scission at constant tension - An example of force-induced collective behaviour. *Epl* **2011**, *94*, 48003.
(118) Zaccone, A.; Terentjev, I.; Di Michele, L.; Terentjev, E. M. Fragmentation and depolymerization of non-covalently bonded filaments. *J. Chem. Phys.* **2015**, *142*, 114905.
(119) Brückner, S.; Allegra, G.; Corradini, P. Helix inversions in polypropylene and polystyrene. *Macromolecules* **2002**, *35*, 3928−3936.
(120) Maeda, N.; Chen, N.; Tirrell, M.; Israelachvili, J. N. Adhesion and Friction Mechanisms of Polymer-on-Polymer Surfaces. *Science* **2002**, *297*, 379−382.
(121) Allegra, G.; Raos, G. Sliding friction between polymer surfaces: a molecular interpretation. *J. Chem. Phys.* **2006**, *124*, 144713.
(122) Jarzynski, C. Nonequilibrium Equality for Free Energy Differences. *Phys. Rev. Lett.* **1997**, *78*, 2690−2693.
(123) Nunes-Alves, A.; Arantes, G. M. Mechanical Unfolding of Macromolecules Coupled to Bond Dissociation. *J. Chem. Theory Comput.* **2018**, *14*, 282−290.
(124) Allen, M. P.; Tildesley, D. J. *Computer simulation of liquids*, 2nd ed.; Oxford University Press, 2017.
(125) Frenkel, D.; Smit, B. *Understanding molecular simulation: From algorithms to applications*. 2002.
(126) Todd, B. D.; Daivis, P. J. *Nonequilibrium molecular dynamics: theory, algorithms and applications*; Cambridge University Press, 2017.
(127) Car, R.; Parrinello, M. Unified Approach for Molecular Dynamics and Density-Functional Theory. *Phys. Rev. Lett.* **1985**, *55*, 2471−2474.
(128) Kohn, W.; Becke, A. D.; Parr, R. G. Density Functional Theory of Electronic Structure. *J. Phys. Chem.* **1996**, *100*, 12974−12980.
(129) Kühne, T. D.; et al. CP2K: An electronic structure and molecular dynamics software package - Quickstep: Efficient and accurate electronic structure calculations. *J. Chem. Phys.* **2020**, *152*, 194103.
(130) Mian, S. A.; Yang, L.-M.; Saha, L. C.; Ahmed, E.; Ajmal, M.; Ganz, E. A Fundamental Understanding of Catechol and Water Adsorption on a Hydrophilic Silica Surface: Exploring the Underwater Adhesion Mechanism of Mussels on an Atomic Scale. *Langmuir* **2014**, *30*, 6906−6914.
(131) Rimola, A.; Costa, D.; Sodupe, M.; Lambert, J.-F.; Ugliengo, P. Silica Surface Features and Their Role in the Adsorption of Biomolecules: Computational Modeling and Experiments. *Chem. Rev.* **2013**, *113*, 4216−4313.
(132) Saitta, A. M.; Klein, M. L. Polyethylene under tensil load: Strain energy storage and breaking of linear and knotted alkanes probed by first-principles molecular dynamics calculations. *J. Chem. Phys.* **1999**, *111*, 9434−9440.
(133) Mattsson, T. R.; Lane, J. M. D.; Cochrane, K. R.; Desjarlais, M. P.; Thompson, A. P.; Pierce, F.; Grest, G. S. First-principles and classical molecular dynamics simulation of shocked polymers. *Phys. Rev. B: Condens. Matter Mater. Phys.* **2010**, *81*, 1−9.
(134) Nouranian, S.; Gwaltney, S. R.; Baskes, M. I.; Tschopp, M. A.; Horstemeyer, M. F. Simulations of tensile bond rupture in single alkane molecules using reactive interatomic potentials. *Chem. Phys. Lett.* **2015**, *635*, 278−284.
(135) Dunning, T. H.; Xu, L. T.; Cooper, D. L.; Karadakov, P. B. Spin-Coupled Generalized Valence Bond Theory: New Perspectives on the Electronic Structure of Molecules and Chemical Bonds. *J. Phys. Chem. A* **2021**, *125*, 2021−2050.
(136) Plimpton, S. Fast parallel algorithms for short-range molecular dynamics. *J. Comput. Phys.* **1995**, *117*, 1−19.
(137) Emami, F. S.; Puddu, V.; Berry, R. J.; Varshney, V.; Patwardhan, S. V.; Perry, C. C.; Heinz, H. Force Field and a Surface Model Database for Silica to Simulate Interfacial Properties in Atomic Resolution. *Chem. Mater.* **2014**, *26*, 2647−2658.
(138) David, A.; Pasquini, M.; Tartaglino, U.; Raos, G. A Coarse-Grained Force Field for Silica−Polybutadiene Interfaces and Nanocomposites. *Polymers* **2020**, *12*, 1484.
(139) Ponder, J. W.; Case, D. A. Force Fields for Protein Simulations. *Adv. Protein Chem.* **2003**, *66*, 27−85.
(140) Senftle, T. P.; Hong, S.; Islam, M. M.; Kylasa, S. B.; Zheng, Y.; Shin, Y. K.; Junkermeier, C.; Engel-Herbert, R.; Janik, M. J.; Aktulga, H. M.; Verstraelen, T.; Grama, A.; van Duin, A. C. T. The ReaxFF reactive force-field: development, applications and future directions. *npj Computational Materials* **2016**, *2*, 15011.
(141) Stuart, S. J.; Tutein, A. B.; Harrison, J. A. A reactive potential for hydrocarbons with intermolecular interactions. *J. Chem. Phys.* **2000**, *112*, 6472−6486.
(142) O'Connor, T. C.; Andzelm, J.; Robbins, M. O. AIREBO-M: A reactive model for hydrocarbons at extreme pressures. *J. Chem. Phys.* **2015**, *142*, 024903.
(143) Liang, T.; Shan, T.-r.; Cheng, Y.-t.; Devine, B. D.; Noordhoek, M.; Li, Y.; Lu, Z.; Phillpot, S. R.; Sinnott, S. B. Classical atomistic simulations of surfaces and heterogeneous interfaces with the charge-optimized many body (COMB) potentials. *Mater. Sci. Eng., R* **2013**, *74*, 255−279.
(144) Behler, J. Perspective: Machine learning potentials for atomistic simulations. *J. Chem. Phys.* **2016**, *145*, 170901.
(145) Friederich, P.; Häse, F.; Proppe, J.; Aspuru-Guzik, A. Machine-learned potentials for next-generation matter simulations. *Nat. Mater.* **2021**, *20*, 750−761.
(146) Pizzi, G.; Cepellotti, A.; Sabatini, R.; Marzari, N.; Kozinsky, B. AiiDA: automated interactive infrastructure and database for computational science. *Comput. Mater. Sci.* **2016**, *111*, 218−230.
(147) Plimpton, S. J.; Thompson, A. P. Computational aspects of many-body potentials. *MRS Bull.* **2012**, *37*, 513−521.
(148) Vashisth, A.; Ashraf, C.; Zhang, W.; Bakis, C. E.; Van Duin, A. C. Accelerated ReaxFF Simulations for Describing the Reactive Cross-Linking of Polymers. *J. Phys. Chem. A* **2018**, *122*, 6633−6642.
(149) Meißner, R. H.; Konrad, J.; Boll, B.; Fiedler, B.; Zahn, D. Molecular simulation of thermosetting polymer hardening: Reactive events enabled by controlled topology transfer. *Macromolecules* **2020**, *53*, 9698−9705.
(150) Kallivokas, S. V.; Sgouros, A. P.; Theodorou, D. N. Molecular dynamics simulations of EPON-862/DETDA epoxy networks: structure, topology, elastic constants, and local dynamics. *Soft Matter* **2019**, *15*, 721−733.
(151) Schichtel, J. J.; Chattopadhyay, A. Modeling thermoset polymers using an improved molecular dynamics crosslinking methodology. *Comput. Mater. Sci.* **2020**, *174*, 109469.

(152) Gissinger, J. R.; Jensen, B. D.; Wise, K. E. Reacter: A heuristic method for reactive molecular dynamics. *Macromolecules* **2020**, *53*, 9953−9961.
(153) Vashisth, A.; Ashraf, C.; Bakis, C. E.; van Duin, A. C. Effect of chemical structure on thermo-mechanical properties of epoxy polymers: Comparison of accelerated ReaxFF simulations and experiments. *Polymer* **2018**, *158*, 354−363.
(154) Buell, S.; Van Vliet, K. J.; Rutledge, G. C. Mechanical Properties of Glassy Polyethylene Nanofibers via Molecular Dynamics Simulations. *Macromolecules* **2009**, *42*, 4887−4895.
(155) Müller-Plathe, F. Coarse-Graining in Polymer Simulation: From the Atomistic to the Mesoscopic Scale and Back. *ChemPhysChem* **2002**, *3*, 754−769.
(156) Peter, C.; Kremer, K. Multiscale simulation of soft matter systems − from the atomistic to the coarse-grained level and back. *Soft Matter* **2009**, *5*, 4357.
(157) Gartner, T. E.; Jayaraman, A. Modeling and Simulations of Polymers: A Roadmap. *Macromolecules* **2019**, *52*, 755−786.
(158) Field, M. J. An Algorithm for Adaptive QC/MM Simulations. *J. Chem. Theory Comput.* **2017**, *13*, 2342−2351.
(159) Praprotnik, M.; Cortes-Huerto, R.; Potestio, R.; Delle Site, L. *Handbook of Materials Modeling*; Springer International Publishing: Cham, 2020; pp 1443−1457, DOI: 10.1007/978-3-319-44677-6_89.
(160) Bernaschi, M.; Melchionna, S.; Succi, S. Mesoscopic simulations at the physics-chemistry-biology interface. *Rev. Mod. Phys.* **2019**, *91*, 25004.
(161) Rahimi, M.; Karimi-Varzaneh, H. A.; Böhm, M. C.; Müller-Plathe, F.; Pfaller, S.; Possart, G.; Steinmann, P. Nonperiodic stochastic boundary conditions for molecular dynamics simulations of materials embedded into a continuum mechanics domain. *J. Chem. Phys.* **2011**, *134*, 154108.
(162) Murashima, T.; Urata, S.; Li, S. Coupling finite element method with large scale atomic/molecular massively parallel simulator (LAMMPS) for hierarchical multiscale simulations. *Eur. Phys. J. B* **2019**, *92*, 211.
(163) David, A.; De Nicola, A.; Tartaglino, U.; Milano, G.; Raos, G. Viscoelasticity of Short Polymer Liquids from Atomistic Simulations. *J. Electrochem. Soc.* **2019**, *166*, B3246−B3256.
(164) Dunbar, M.; Keten, S. Energy Renormalization for Coarse-Graining a Biomimetic Copolymer, Poly(catechol-styrene). *Macromolecules* **2020**, *53*, 9397−9405.
(165) Yang, S.; Cui, Z.; Qu, J. A coarse-grained model for epoxy molding compound. *J. Phys. Chem. B* **2014**, *118*, 1660−1669.
(166) Tsige, M.; Stevens, M. J. Effect of cross-linker functionality on the adhesion of highly cross-linked polymer networks: A molecular dynamics study of epoxies. *Macromolecules* **2004**, *37*, 630−637.
(167) Yang, S.; Qu, J. Coarse-grained molecular dynamics simulations of the tensile behavior of a thermosetting polymer. *Phys. Rev. E* **2014**, *90*, 012601.
(168) Baggioli, A.; Casalegno, M.; David, A.; Pasquini, M.; Raos, G. Polymer-Mediated Adhesion: Nanoscale Surface Morphology and Failure Mechanisms. *Macromolecules* **2021**, *54*, 195−202.
(169) Kremer, K.; Grest, G. S. Dynamics of entangled linear polymer melts: A molecular-dynamics simulation. *J. Chem. Phys.* **1990**, *92*, 5057−5086.
(170) Everaers, R.; Karimi-Varzaneh, H. A.; Fleck, F.; Hojdis, N.; Svaneborg, C. Kremer−Grest Models for Commodity Polymer Melts: Linking Theory, Experiment, and Simulation at the Kuhn Scale. *Macromolecules* **2020**, *53*, 1901−1916.
(171) Ronca, G.; Allegra, G. An approach to rubber elasticity with internal constraints. *J. Chem. Phys.* **1975**, *63*, 4990−4997.
(172) Rottach, D. R.; Curro, J. G.; Budzien, J.; Grest, G. S.; et al. Permanent Set of Cross-Linking Networks: Comparison of Theory with Molecular Dynamics Simulations. *Macromolecules* **2006**, *39*, 5521−5530.
(173) Allegra, G.; Raos, G.; Vacatello, M. Theories and simulations of polymer-based nanocomposites: From chain statistics to reinforcement. *Prog. Polym. Sci.* **2008**, *33*, 683−731.
(174) Hagita, K.; Morita, H.; Doi, M.; Takano, H. Coarse-Grained Molecular Dynamics Simulation of Filled Polymer Nanocomposites under Uniaxial Elongation. *Macromolecules* **2016**, *49*, 1972−1983.
(175) Pasquini, M.; Raos, G. Tunable interaction potentials and morphology of polymer−nanoparticle blends. *J. Chem. Phys.* **2020**, *152*, 174902.
(176) Gersappe, D.; Robbins, M. O. Where do polymer adhesives fail? *Europhys. Lett.* **1999**, *48*, 150−155.
(177) Froltsov, V. A.; Klüppel, M.; Raos, G. Molecular dynamics simulation of rupture in glassy polymer bridges within filler aggregates. *Phys. Rev. E* **2012**, *86*, 041801.
(178) Solar, M.; Qin, Z.; Buehler, M. J. Molecular mechanics and performance of crosslinked amorphous polymer adhesives. *J. Mater. Res.* **2014**, *29*, 1077−1085.
(179) Jin, K.; López Barreiro, D.; Martin-Martinez, F. J.; Qin, Z.; Hamm, M.; Paul, C. W.; Buehler, M. J. Improving the performance of pressure sensitive adhesives by tuning the crosslinking density and locations. *Polymer* **2018**, *154*, 164−171.
(180) Pastore, R.; David, A.; Casalegno, M.; Greco, F.; Raos, G. Influence of wall heterogeneity on nanoscopically confined polymers. *Phys. Chem. Chem. Phys.* **2019**, *21*, 772−779.
(181) Stevens, M. J. Interfacial fracture between highly cross-linked polymer networks and a solid surface: Effect of interfacial bond density. *Macromolecules* **2001**, *34*, 2710−2718.
(182) Sides, S. W.; Grest, G. S.; Stevens, M. J. Large-Scale Simulation of Adhesion Dynamics for End-Grafted Polymers. *Macromolecules* **2002**, *35*, 566−573.
(183) Ge, T.; Pierce, F.; Perahia, D.; Grest, G. S.; Robbins, M. O. Molecular Dynamics Simulations of Polymer Welding: Strength from Interfacial Entanglements. *Phys. Rev. Lett.* **2013**, *110*, 098301.
(184) Sliozberg, Y. R.; Hoy, R. S.; Mrozek, R. A.; Lenhart, J. L.; Andzelm, J. W. Role of entanglements and bond scission in high strain-rate deformation of polymer gels. *Polymer* **2014**, *55*, 2543−2551.
(185) Wan, H.; Gao, K.; Li, S.; Zhang, L.; Wu, X.; Wang, X.; Liu, J. Chemical Bond Scission and Physical Slippage in the Mullins Effect and Fatigue Behavior of Elastomers. *Macromolecules* **2019**, *52*, 4209−4221.
(186) Nabavi, S. S.; Fratzl, P.; Hartmann, M. a. Energy dissipation and recovery in a simple model with reversible cross-links. *Phys. Rev. E* **2015**, *91*, 1−9.
(187) Baljon, A. R.; Robbins, M. O. A molecular view of bond rupture. *Comput. Theor. Polym. Sci.* **1999**, *9*, 35−40.
(188) Robbins, M.; Müser, M. *Modern Tribology Handbook: Vol. One*; Principles of Tribology, 2000; pp 717−765, DOI: 10.1201/9780849377877.ch20.
(189) Baljon, A. R. C.; Robbins, M. O. Simulations of crazing in polymer glasses: Effect of chain length and surface tension. *Macromolecules* **2001**, *34*, 4200−4209.
(190) Rottler, J.; Robbins, M. O. Growth, microstructure, and failure of crazes in glassy polymers. *Phys. Rev. E: Stat. Phys., Plasmas, Fluids, Relat. Interdiscip. Top.* **2003**, *68*, 18.
(191) Baljon, A. R. C.; Vorselaars, J.; Depuy, T. J. Computational Studies of Contact Time Dependence of Adhesive Energy Due to Redistribution of the Locations of Strong Specific Interfacial Interactions. *Macromolecules* **2004**, *37*, 5800−5806.
(192) Pastewka, L.; Robbins, M. O. Contact between rough surfaces and a criterion for macroscopic adhesion. *Proc. Natl. Acad. Sci. U. S. A.* **2014**, *111*, 3298−3303.
(193) Benz, M.; Rosenberg, K. J.; Kramer, E. J.; Israelachvili, J. N. The Deformation and Adhesion of Randomly Rough and Patterned Surfaces. *J. Phys. Chem. B* **2006**, *110*, 11884−11893.
(194) Zappone, B.; Rosenberg, K. J.; Israelachvili, J. Role of nanometer roughness on the adhesion and friction of a rough polymer surface and a molecularly smooth mica surface. *Tribol. Lett.* **2007**, *26*, 191.
(195) Fuller, K. N. G.; Tabor, D. The effect of surface roughness on the adhesion of elastic solids. *Proc. R. Soc. London, Ser. A* **1975**, *345*, 327−342.

https://doi.org/10.1021/acs.macromol.1c01182
Macromolecules 2021, 54, 10617−10644

(196) Archard, J. F.; Allibone, T. E. Elastic deformation and the laws of friction. *Proceedings of the Royal Society of London. Series A* **1957**, *243*, 190−205.
(197) Greenwood, J. A.; Williamson, J. B. P.; Bowden, F. P. Contact of nominally flat surfaces. *Proceedings of the Royal Society of London. Series A. Mathematical and Physical Sciences* **1966**, *295*, 300−319.
(198) Mandelbrot, B. B.; Passoja, D. E.; Paullay, A. J. Fractal character of fracture surfaces of metals. *Nature* **1984**, *308*, 721−722.
(199) Majumdar, A.; Bhushan, B. Fractal Model of Elastic-Plastic Contact Between Rough Surfaces. *J. Tribol.* **1991**, *113*, 1−11.
(200) Bhushan, B. Contact mechanics of rough surfaces in tribology: multiple asperity contact. *Tribol. Lett.* **1998**, *4*, 1−35.
(201) Persson, B. N. J.; Tosatti, E. Qualitative theory of rubber friction and wear. *J. Chem. Phys.* **2000**, *112*, 2021−2029.
(202) Persson, B. N. J.; Tosatti, E. The effect of surface roughness on the adhesion of elastic solids. *J. Chem. Phys.* **2001**, *115*, 5597−5610.
(203) Yang, C.; Persson, B. N. J. Contact mechanics: contact area and interfacial separation from small contact to full contact. *J. Phys.: Condens. Matter* **2008**, *20*, 215214.
(204) Persson, B. N. J.; Scaraggi, M. Theory of adhesion: Role of surface roughness. *J. Chem. Phys.* **2014**, *141*, 124701.
(205) Campana, C.; Mueser, M. H.; Robbins, M. O. Elastic contact between self-affine surfaces: comparison of numerical stress and contact correlation functions with analytic predictions. *J. Phys.: Condens. Matter* **2008**, *20*, 354013.
(206) Hyun, S.; Pei, L.; Molinari, J.-F.; Robbins, M. O. Finite-element analysis of contact between elastic self-affine surfaces. *Phys. Rev. E* **2004**, *70*, 026117.
(207) Yastrebov, V. A.; Anciaux, G.; Molinari, J.-F. m. c. Contact between representative rough surfaces. *Phys. Rev. E* **2012**, *86*, 035601.
(208) Pastewka, L.; Robbins, M. O. Contact between rough surfaces and a criterion for macroscopic adhesion. *Proc. Natl. Acad. Sci. U. S. A.* **2014**, *111*, 3298−3303.
(209) Gujrati, A.; Khanal, S. R.; Pastewka, L.; Jacobs, T. D. B. Combining TEM, AFM, and Profilometry for Quantitative Topography Characterization Across All Scales. *ACS Appl. Mater. Interfaces* **2018**, *10*, 29169−29178.
(210) Dalvi, S.; Gujrati, A.; Khanal, S. R.; Pastewka, L.; Dhinojwala, A.; Jacobs, T. D. B. Linking energy loss in soft adhesion to surface roughness. *Proc. Natl. Acad. Sci. U. S. A.* **2019**, *116*, 25484−25490.
(211) Bettscheider, S.; Gachot, C.; Rosenkranz, A. How to measure the real contact area? A simple marker and relocation foot-printing approach. *Tribol. Int.* **2016**, *103*, 167−175.
(212) Weber, B.; Suhina, T.; Junge, T.; Pastewka, L.; Brouwer, A. M.; Bonn, D. Molecular probes reveal deviations from Amontons' law in multi-asperity frictional contacts. *Nat. Commun.* **2018**, *9*, 888.
(213) Autumn, K.; Liang, Y. A.; Hsieh, S. T.; Zesch, W.; Chan, W. P.; Kenny, T. W.; Fearing, R.; Full, R. J. Adhesive force of a single gecko foot-hair. *Nature* **2000**, *405*, 681−685.
(214) Arzt, E.; Gorb, S.; Spolenak, R. From micro to nano contacts in biological attachment devices. *Proc. Natl. Acad. Sci. U. S. A.* **2003**, *100*, 10603−10606.
(215) Boesel, L. F.; Greiner, C.; Arzt, E.; del Campo, A. Gecko-Inspired Surfaces: A Path to Strong and Reversible Dry Adhesives. *Adv. Mater.* **2010**, *22*, 2125−2137.
(216) Israelachvili, J.; Min, Y.; Akbulut, M.; Alig, A.; Carver, G.; Greene, W.; Kristiansen, K.; Meyer, E.; Pesika, N.; Rosenberg, K.; et al. Recent advances in the surface forces apparatus (SFA) technique. *Rep. Prog. Phys.* **2010**, *73*, 036601.
(217) Butt, H.-J.; Cappella, B.; Kappl, M. Force measurements with the atomic force microscope: Technique, interpretation and applications. *Surf. Sci. Rep.* **2005**, *59*, 1−152.
(218) Wang, M. D.; Yin, H.; Landick, R.; Gelles, J.; Block, S. M. Stretching DNA with optical tweezers. *Biophys. J.* **1997**, *72*, 1335−1346.
(219) Neuman, K. C.; Nagy, A. Single-molecule force spectroscopy: optical tweezers, magnetic tweezers and atomic force microscopy. *Nat. Methods* **2008**, *5*, 491−505.
(220) Gao, D.; Ding, W.; Nieto-Vesperinas, M.; Ding, X.; Rahman, M.; Zhang, T.; Lim, C. T.; Qiu, C.-W. Optical manipulation from the microscale to the nanoscale: fundamentals, advances and prospects. *Light: Sci. Appl.* **2017**, *6*, e17039−e17039.
(221) Israelachvili, J. N. Thin film studies using multiple-beam interferometry. *J. Colloid Interface Sci.* **1973**, *44*, 259−272.
(222) Israelachvili, J. N.; Tandon, R. K.; White, L. R. Measurement of forces between two mica surfaces in aqueous poly(ethylene oxide) solutions. *Nature* **1979**, *277*, 120−121.
(223) Klein, J. Forces between mica surfaces bearing layers of adsorbed polystyrene in cyclohexane. *Nature* **1980**, *288*, 248−250.
(224) Israelachvili, J. N.; Tirrell, M.; Klein, J.; Almog, Y. Forces between two layers of adsorbed polystyrene immersed in cyclohexane below and above the temperature. *Macromolecules* **1984**, *17*, 204.
(225) Klein, J.; Luckham, P. F. Long-range attractive forces between two mica surfaces in an aqueous polymer solution. *Nature* **1984**, *308*, 836−837.
(226) Klein, J.; Luckham, P. F. Forces between two adsorbed poly(ethylene oxide) layers in a good aqueous solvent in the range 0−150 nm. *Macromolecules* **1984**, *17*, 1041−1048.
(227) Hadziioannou, G.; Patel, S.; Granick, S.; Tirrell, M. Forces between surfaces of block copolymers adsorbed on mica. *J. Am. Chem. Soc.* **1986**, *108*, 2869−2876.
(228) Taunton, H.; Toprakcioglu, C.; Fetters, L. J.; Klein, J. Forces between surfaces bearing terminally anchored polymer chains in good solvents. *Nature* **1988**, *332*, 712−714.
(229) Taunton, H. J.; Toprakcioglu, C.; Fetters, L. J.; Klein, J. Interactions between surfaces bearing end-adsorbed chains in a good solvent. *Macromolecules* **1990**, *23*, 571.
(230) Watanabe, H.; Tirrell, M. Measurement of forces in symmetric and asymmetric interactions between diblock copolymer layers adsorbed on mica. *Macromolecules* **1993**, *26*, 6455−6466.
(231) Tirrell, M.; Patel, S.; Hadziioannou, G. Polymeric Amphiphiles at Solid-Fluid Interfaces: Forces between Layers of Adsorbed Block Copolymers. *Proc. Natl. Acad. Sci. U. S. A.* **1987**, *84*, 4725−4728.
(232) Dai, L.; Toprakcioglu, C. End-adsorbed triblock copolymer chains at the liquid-solid interface: bridging effects in a good solvent. *Macromolecules* **1992**, *25*, 6000−6006.
(233) Zappone, B.; Ruths, M.; Greene, G. W.; Jay, G. D.; Israelachvili, J. N. Adsorption, Lubrication, and Wear of Lubricin on Model Surfaces: Polymer Brush-Like Behavior of a Glycoprotein. *Biophys. J.* **2007**, *92*, 1693.
(234) Hammer, D. A.; Tirrell, M. Biological Adhesion at Interfaces. *Annu. Rev. Mater. Sci.* **1996**, *26*, 651−691.
(235) Wong, J. Y.; Kuhl, T. L.; Israelachvili, J. N.; Mullah, N.; Zalipsky, S. Direct measurement of a tethered ligand-receptor interaction potential. *Science* **1997**, *275*, 820−2.
(236) Leckband, D.; Israelachvili, J. Intermolecular forces in biology. *Q. Rev. Biophys.* **2001**, *34*, 105−267.
(237) Balastre, M.; Li, F.; Schorr, P.; Yang, J.; Mays, J. W.; Tirrell, M. V. A study of polyelectrolyte brushes formed from adsorption of amphiphilic diblock copolymers using the surface forces apparatus. *Macromolecules* **2002**, *35*, 9480.
(238) Raviv, U.; Giasson, S.; Kampf, N.; Gohy, J. F.; Jérôme, R.; Klein, J. Lubrication by charged polymers. *Nature* **2003**, *425*, 163.
(239) Claesson, P. M.; Poptoshev, E.; Blomberg, E.; Dedinaite, A. Polyelectrolyte-mediated surface interactions. *Adv. Colloid Interface Sci.* **2005**, *114*−*115*, 173−87.
(240) Chen, M.; Briscoe, W. H.; Armes, S. P.; Klein, J. Lubrication at Physiological Pressures by Polyzwitterionic Brushes. *Science* **2009**, *323*, 1698−1701.
(241) Luckham, P. F.; Klein, J. Forces between mica surfaces bearing adsorbed polyelectrolyte, poly-L-lysine, in aqueous media. *J. Chem. Soc., Faraday Trans. 1* **1984**, *80*, 865−878.
(242) Farina, R.; Laugel, N.; Yu, J.; Tirrell, M. Reversible Adhesion with Polyelectrolyte Brushes Tailored via the Uptake and Release of Trivalent Lanthanum Ions. *J. Phys. Chem. C* **2015**, *119*, 14805−14814.

https://doi.org/10.1021/acs.macromol.1c01182
Macromolecules 2021, 54, 10617−10644

(243) Yu, J.; Jackson, N. E.; Xu, X.; Morgenstern, Y.; Kaufman, Y.; Ruths, M.; de Pablo, J. J.; Tirrell, M. Multivalent counterions diminish the lubricity of polyelectrolyte brushes. *Science* **2018**, *360*, 1434−1438.
(244) Ducker, W. A.; Senden, T. J.; Pashley, R. M. Direct measurement of colloidal forces using an atomic force microscope. *Nature* **1991**, *353*, 239−241.
(245) Strick, T. R.; Dessinges, M. N.; Charvin, G.; Dekker, N. H.; Allemand, J. F.; Bensimon, D.; Croquette, V. Stretching of macromolecules and proteins. *Rep. Prog. Phys.* **2003**, *66*, 1−45.
(246) Neuman, K. C.; Nagy, A. Single-molecule force spectroscopy: optical tweezers, magnetic tweezers and atomic force microscopy. *Nat. Methods* **2008**, *5*, 491−505.
(247) Hughes, M. L.; Dougan, L. The physics of pulling polyproteins: a review of single molecule force spectroscopy using the AFM to study protein unfolding. *Rep. Prog. Phys.* **2016**, *79*, 076601.
(248) Luo, Z.; Zhang, A.; Chen, Y.; Shen, Z.; Cui, S. How Big Is Big Enough? Effect of Length and Shape of Side Chains on the Single-Chain Enthalpic Elasticity of a Macromolecule. *Macromolecules* **2016**, *49*, 3559−3565.
(249) Bao, Y.; Qian, H.-J.; Lu, Z.-Y.; Cui, S. The unexpected flexibility of natural cellulose at a single-chain level and its implications to the design of nano materials. *Nanoscale* **2014**, *6*, 13421−13424.
(250) Hugel, T.; Rief, M.; Seitz, M.; Gaub, H. E.; Netz, R. R. Highly stretched single polymers: Atomic-force-microscope experiments versus ab-initio theory. *Phys. Rev. Lett.* **2005**, *94*, 048301 DOI: 10.1103/PhysRevLett.94.048301.
(251) Cheng, B.; Wu, S.; Liu, S.; Rodriguez-Aliaga, P.; Yu, J.; Cui, S. Protein denaturation at a single-molecule level: the effect of nonpolar environments and its implications on the unfolding mechanism by proteases. *Nanoscale* **2015**, *7*, 2970−2977.
(252) Hinterdorfer, P.; Baumgartner, W.; Gruber, H. J.; Schilcher, K.; Schindler, H. Detection and localization of individual antibody-antigen recognition events by atomic force microscopy. *Proc. Natl. Acad. Sci. U. S. A.* **1996**, *93*, 3477−3481.
(253) Merkel, R.; Nassoy, P.; Leung, A.; Ritchie, K.; Evans, E. Energy landscapes of receptor-ligand bonds explored with dynamic force spectroscopy. *Nature* **1999**, *397*, 50−53.
(254) Grandbois, M.; Beyer, M.; Rief, M.; Clausen-Schaumann, H.; Gaub, H. E. How strong is a covalent bond? *Science* **1999**, *283*, 1727−1730.
(255) Lin, Q.; Gourdon, D.; Sun, C. J.; Holten-Andersen, N.; Anderson, T. H.; Waite, J. H.; Israelachvili, J. N. Adhesion mechanisms of the mussel foot proteins mfp-1 and mfp-3. *Proc. Natl. Acad. Sci. U. S. A.* **2007**, *104*, 3782−3786.
(256) Steinbauer, P.; Rohatschek, A.; Andriotis, O.; Bouropoulos, N.; Liska, R.; Thurner, P. J.; Baudis, S. Single-Molecule Force Spectroscopy Reveals Adhesion-by-Demand in Statherin at the Protein−Hydroxyapatite Interface. *Langmuir* **2020**, *36*, 13292−13300.
(257) Lee, B. P.; Messersmith, P. B.; Israelachvili, J. N.; Waite, J. H. Mussel-inspired adhesives and coatings. *Annu. Rev. Mater. Res.* **2011**, *41*, 99−132.
(258) Smith, B. L.; Schaffer, T. E.; Viani, M.; Thompson, J. B.; Frederick, N. A.; Kindt, J.; Belcher, A.; Stucky, G. D.; Morse, D. E.; Hansma, P. K. Molecular mechanistic origin of the toughness of natural adhesives, fibres and composites. *Nature* **1999**, *399*, 761−763.
(259) Thompson, J. B.; Kindt, J. H.; Drake, B.; Hansma, H. G.; Morse, D. E.; Hansma, P. K. Bone indentation recovery time correlates with bond reforming time. *Nature* **2001**, *414*, 773−776.
(260) Fantner, G. E.; Hassenkam, T.; Kindt, J. H.; Weaver, J. C.; Birkedal, H.; Pechenik, L.; Cutroni, J. A.; Cidade, G. A. G.; Stucky, G. D.; Morse, D. E.; Hansma, P. K. Sacrificial bonds and hidden length dissipate energy as mineralized fibrils separate during bone fracture. *Nat. Mater.* **2005**, *4*, 612−616.
(261) Zappone, B.; Thurner, P. J.; Adams, J.; Fantner, G. E.; Hansma, P. K. Effect of Ca2+ ions on the adhesion and mechanical properties of adsorbed layers of human osteopontin. *Biophys. J.* **2008**, *95*, 2939−2950.
(262) Hugel, T.; Holland, N. B.; Cattani, A.; Moroder, L.; Seitz, M.; Gaub, H. E. Single-Molecule Optomechanical Cycle. *Science* **2002**, *296*, 1103−1106.
(263) Wu, J.; Li, P.; Dong, C.; Jiang, H.; Bin, X.; Gao, X.; Qin, M.; Wang, W.; Bin, C.; Cao, Y. Rationally designed synthetic protein hydrogels with predictable mechanical properties. *Nat. Commun.* **2018**, *9*, 620.
(264) Lin, Q.; Gourdon, D.; Sun, C. J.; Holten-Andersen, N.; Anderson, T. H.; Waite, J. H.; Israelachvili, J. N. Adhesion mechanisms of the mussel foot proteins mfp-1 and mfp-3. *Proc. Natl. Acad. Sci. U. S. A.* **2007**, *104*, 3782−3786.
(265) Campbell, D.; Pethrick, R. A.; White, J. R. *Polymer characterization: Physical techniques*, 2nd ed.; Stanley Thornes Ltd.: Cheltenham, U.K., 2000.
(266) Stamm, M. *Polymer Surfaces and Interfaces: Characterization, Modification and Applications*; Springer: Dresden, Germany, 2008.
(267) Petrone, L.; Kumar, A.; Sutanto, C. N.; Patil, N. J.; Kannan, S.; Palaniappan, A.; Amini, S.; Zappone, B.; Verma, C.; Miserez, A. Mussel adhesion is dictated by time-regulated secretion and molecular conformation of mussel adhesive proteins. *Nat. Commun.* **2015**, *6*, 8737.
(268) Mathis, C. H.; Divandari, M.; Simic, R.; Naik, V. V.; Benetti, E. M.; Isa, L.; Spencer, N. D. ATR-IR Investigation of Solvent Interactions with Surface-Bound Polymers. *Langmuir* **2016**, *32*, 7588−7595.
(269) Damin, C. A.; Nguyen, V. H. T.; Niyibizi, A. S.; Smith, E. A. Application of scanning angle Raman spectroscopy for determining the location of buried polymer interfaces with tens of nanometer precision. *Analyst* **2015**, *140*, 1955−1964.
(270) Grundmeier, G.; Stratmann, M. Adhesion and de-adhesion mechanisms at polymer/metal interfaces: Mechanistic understanding based on in situ studies of buried interfaces. *Annu. Rev. Mater. Res.* **2005**, *35*, 571−615.
(271) Chen, Z.; Shen, Y. R.; Somorjai, G. A. Studies of polymer surfaces by sum frequency generation vibrational spectroscopy. *Annu. Rev. Phys. Chem.* **2002**, *53*, 437−465.
(272) Williams, C. T.; Beattie, D. A. Probing buried interfaces with non-linear optical spectroscopy. *Surf. Sci.* **2002**, *500*, 545−576.
(273) Zhang, C.; Myers, J. N.; Chen, Z. Elucidation of molecular structures at buried polymer interfaces and biological interfaces using sum frequency generation vibrational spectroscopy. *Soft Matter* **2013**, *9*, 4738−4761.
(274) Tian, C. S.; Shen, Y. R. Recent progress on sum-frequency spectroscopy. *Surf. Sci. Rep.* **2014**, *69*, 105−131.
(275) Wang, H.-F.; Velarde, L.; Gan, W.; Fu, L. Quantitative Sum-Frequency Generation Vibrational Spectroscopy of Molecular Surfaces and Interfaces: Lineshape, Polarization, and Orientation. *Annu. Rev. Phys. Chem.* **2015**, *66*, 189−216.
(276) Lu, X.; Zhang, C.; Ulrich, N.; Xiao, M.; Ma, Y.-H.; Chen, Z. Studying Polymer Surfaces and Interfaces with Sum Frequency Generation Vibrational Spectroscopy. *Anal. Chem.* **2017**, *89*, 466−489.
(277) Pagliusi, P.; Chen, C. Y.; Shen, Y. R. Molecular orientation and alignment of rubbed poly(vinyl cinnamate) surfaces. *J. Chem. Phys.* **2006**, *125*, 201104.
(278) Yurdumakan, B.; Nanjundiah, K.; Dhinojwala, A. Origin of Higher Friction for Elastomers Sliding on Glassy Polymers. *J. Phys. Chem. C* **2007**, *111*, 960−965.
(279) Defante, A. P.; Nyarko, A.; Kaur, S.; Burai, T. N.; Dhinojwala, A. Interstitial Water Enhances Sliding Friction. *Langmuir* **2018**, *34*, 4084−4094.
(280) Kaur, S.; Wilson, M. C.; Dhinojwala, A. In *Macromolecular Engineering*; Lubnin, A., Erdodi, G., Eds.; Elsevier, 2021; pp 257−276, DOI: 10.1016/B978-0-12-821998-0.00013-2.
(281) Myers, J. N.; Zhang, C.; Lee, K.-W.; Williamson, J.; Chen, Z. Hygrothermal Aging Effects on Buried Molecular Structures at Epoxy Interfaces. *Langmuir* **2014**, *30*, 165−171.
(282) Leng, C.; Liu, Y.; Jenkins, C.; Meredith, H.; Wilker, J. J.; Chen, Z. Interfacial Structure of a DOPA-Inspired Adhesive Polymer Studied by Sum Frequency Generation Vibrational Spectroscopy. *Langmuir* **2013**, *29*, 6659−6664.

(283) Zhang, C.; Jasensky, J.; Leng, C.; Del Grosso, C.; Smith, G. D.; Wilker, J. J.; Chen, Z. Sum frequency generation vibrational spectroscopic studies on buried heterogeneous biointerfaces. *Opt. Lett.* **2014**, *39*, 2715−2718.
(284) Singla, S.; Amarpuri, G.; Dhopatkar, N.; Blackledge, T. A.; Dhinojwala, A. Hygroscopic compounds in spider aggregate glue remove interfacial water to maintain adhesion in humid conditions. *Nat. Commun.* **2018**, *9*, 1890.
(285) Kaur, S.; Narayanan, A.; Dalvi, S.; Liu, Q.; Joy, A.; Dhinojwala, A. Direct Observation of the Interplay of Catechol Binding and Polymer Hydrophobicity in a Mussel-Inspired Elastomeric Adhesive. *ACS Cent. Sci.* **2018**, *4*, 1420−1429.
(286) Narayanan, A.; Kaur, S.; Kumar, N.; Tsige, M.; Joy, A.; Dhinojwala, A. Cooperative Multivalent Weak and Strong Interfacial Interactions Enhance the Adhesion of Mussel-Inspired Adhesives. *Macromolecules* **2021**, *54*, 5417−5428.
(287) Meyer, E. E.; Rosenberg, K. J.; Israelachvili, J. Recent progress in understanding hydrophobic interactions. *Proc. Natl. Acad. Sci. U. S. A.* **2006**, *103*, 15739−15746.
(288) Raffaini, G.; Ganazzoli, F. Protein adsorption on a hydrophobic surface: A molecular dynamics study of lysozyme on graphite. *Langmuir* **2010**, *26*, 5679−5689.
(289) Taboada, G. M.; Yang, K.; Pereira, M. J. N.; Liu, S. S.; Hu, Y.; Karp, M.; Artzi, N.; Lee, Y. Overcoming the translational barriers of tissue adhesives. *Nature Reviews Materials* **2020**, *5*, 310−329.
(290) Furth, M. E.; Atala, A.; Van Dyke, M. E. Smart biomaterials design for tissue engineering and regenerative medicine. *Biomaterials* **2007**, *28*, 5068−5073.
(291) Mano, J. F. Stimuli-responsive polymeric systems for biomedical applications. *Adv. Eng. Mater.* **2008**, *10*, 515−527.
(292) Annabi, N.; Tamayol, A.; Uquillas, J. A.; Akbari, M.; Bertassoni, L. E.; Cha, C.; Camci-Unal, G.; Dokmeci, M. R.; Peppas, N. A.; Khademhosseini, A. 25th Anniversary Article: Rational Design and Applications of Hydrogels in Regenerative Medicine. *Adv. Mater.* **2014**, *26*, 85−124.
(293) Yuk, H.; Zhang, T.; Lin, S.; Parada, G. A.; Zhao, X. Tough bonding of hydrogels to diverse non-porous surfaces. *Nat. Mater.* **2016**, *15*, 190−196.
(294) Young, J. Z.; Medawar, P. B. Fibrin suture of peripheral nerves: Measurement of the rate of regeneration. *Lancet* **1940**, *236*, 126−128.
(295) Faure, E.; Falentin-Daudre, C.; Jerome, C.; Lyskawa, J.; Fournier, D.; Woisel, P.; Detrembleur, C. Catechols as versatile platforms in polymer chemistry. *Prog. Polym. Sci.* **2013**, *38*, 236−270.
(296) Yang, J.; Stuart, M. A. C.; Kamperman, M. Jack of all trades: versatile catechol crosslinking mechanisms. *Chem. Soc. Rev.* **2014**, *43*, 8271−8298.
(297) Moulay, S. Dopa/Catechol-Tethered Polymers: Bioadhesives and Biomimetic Adhesive Materials. *Polym. Rev.* **2014**, *54*, 436−513.
(298) Waite, J. H. Mussel adhesion - essential footwork. *J. Exp. Biol.* **2017**, *220*, 517−530.
(299) Kord Forooshani, P.; Lee, B. P. Recent approaches in designing bioadhesive materials inspired by mussel adhesive protein. *J. Polym. Sci., Part A: Polym. Chem.* **2017**, *55*, 9−33.
(300) Guo, Q.; Chen, J.; Wang, J.; Zeng, H.; Yu, J. Recent progress in synthesis and application of mussel-inspired adhesives. *Nanoscale* **2020**, *12*, 1307−1324.
(301) Barthelat, F.; Yin, Z.; Buehler, M. J. Structure and mechanics of interfaces in biological materials. *Nature Reviews Materials* **2016**, *1*, 16007.
(302) Fantner, G. E.; Adams, J.; Turner, P.; Thurner, P. J.; Fisher, L. W.; Hansma, P. K. Nanoscale Ion Mediated Networks in Bone: Osteopontin Can Repeatedly Dissipate Large Amounts of Energy. *Nano Lett.* **2007**, *7*, 2491−2498.
(303) Saiz-Poseu, J.; Mancebo-Aracil, J.; Nador, F.; Busqué, F.; Ruiz-Molina, D. The chemistry behind catechol-based adhesion. *Angew. Chem., Int. Ed.* **2019**, *58*, 696−714.
(304) Liu, Y. L.; Ai, K. L.; Lu, L. H. Polydopamine and Its Derivative Materials: Synthesis and Promising Applications in Energy, Environmental, and Biomedical Fields. *Chem. Rev.* **2014**, *114*, 5057−5115.
(305) Harrington, M. J.; Masic, A.; Holten-Andersen, N.; Waite, J. H.; Fratzl, P. Iron-Clad Fibers: A Metal-Based Biological Strategy for Hard Flexible Coatings. *Science* **2010**, *328*, 216−220.
(306) Zeng, H. B.; Hwang, D. S.; Israelachvili, J. N.; Waite, J. H. Strong reversible Fe3+-mediated bridging between dopa-containing protein films in water. *Proc. Natl. Acad. Sci. U. S. A.* **2010**, *107*, 12850−12853.
(307) Yount, W. C.; Loveless, D. M.; Craig, S. L. Strong means slow: Dynamic contributions to the bulk mechanical properties of supramolecular networks. *Angew. Chem., Int. Ed.* **2005**, *44*, 2746−2748.
(308) Yang, J.; Saggiomo, V.; Velders, A. H.; Stuart, M. A. C.; Kamperman, M. Reaction pathways in catechol/primary amine mixtures: A window on crosslinking chemistry. *PLoS One* **2016**, *11*, No. e0166490.
(309) Li, L.; Smitthipong, W.; Zeng, H. B. Mussel-inspired hydrogels for biomedical and environmental applications. *Polym. Chem.* **2015**, *6*, 353−358.
(310) Waite, J. H. Translational bioadhesion research: embracing biology without tokenism. *Philos. Trans. R. Soc., B* **2019**, *374*, 20190207.
(311) Endrizzi, B. J.; Stewart, R. J. Glueomics: An Expression Survey of the Adhesive Gland of the Sandcastle Worm. *J. Adhes.* **2009**, *85*, 546−559.
(312) Kan, Y. J.; Danner, E. W.; Israelachvili, J. N.; Chen, Y. F.; Waite, J. H. Boronate Complex Formation with Dopa Containing Mussel Adhesive Protein Retards pH-Induced Oxidation and Enables Adhesion to Mica. *PLoS One* **2014**, *9*, e108869.
(313) Petrone, L.; Kumar, A.; Sutanto, C. N.; Patil, N. J.; Kannan, S.; Palaniappan, A.; Amini, S.; Zappone, B.; Verma, C.; Miserez, A. Mussel adhesion is dictated by time-regulated secretion and molecular conformation of mussel adhesive proteins. *Nat. Commun.* **2015**, *6*, 8737 DOI: 10.1038/ncomms9737.
(314) Maier, G. P.; Rapp, M. V.; Waite, J. H.; Israelachvili, J. N.; Butler, A. Adaptive synergy between catechol and lysine promotes wet adhesion by surface salt displacement. *Science* **2015**, *349*, 628−632.
(315) Wilker, J. J. Redox and adhesion on the rocks. *Nat. Chem. Biol.* **2011**, *7*, 579−580.
(316) Bilotto, P.; Labate, C.; De Santo, M. P.; Deepankumar, K.; Miserez, A.; Zappone, B. Adhesive Properties of Adsorbed Layers of Two Recombinant Mussel Foot Proteins with Different Levels of DOPA and Tyrosine. *Langmuir* **2019**, *35*, 15481−15490.
(317) de Kruif, C. G.; Weinbreck, F.; de Vries, R. Complex coacervation of proteins and anionic polysaccharides. *Curr. Opin. Colloid Interface Sci.* **2004**, *9*, 340−349.
(318) Wang, C. S.; Stewart, R. J. Localization of the bioadhesive precursors of the sandcastle worm, Phragmatopoma californica (Fewkes). *J. Exp. Biol.* **2012**, *215*, 351−361.
(319) Deepankumar, K.; Guo, Q.; Mohanram, H.; Lim, J.; Mu, Y.; Pervushin, K.; Yu, J.; Miserez, A. Liquid−liquid phase separation of the green mussel adhesive protein Pvfp-5 is regulated by the post-translated Dopa amino acid. *Adv. Mater.* **2021**, 2103828.
(320) Wei, W.; Tan, Y. P.; Rodriguez, N. R. M.; Yu, J.; Israelachvili, J. N.; Waite, J. H. A mussel-derived one component adhesive coacervate. *Acta Biomater.* **2014**, *10*, 1663−1670.
(321) Kim, S.; Yoo, H. Y.; Huang, J.; Lee, Y.; Park, S.; Park, Y.; Jin, S.; Jung, Y. M.; Zeng, H. B.; Hwang, D. S.; Jho, Y. Salt Triggers the Simple Coacervation of an Underwater Adhesive When Cations Meet Aromatic pi Electrons in Seawater. *ACS Nano* **2017**, *11*, 6764−6772.
(322) Lim, S.; Choi, Y. S.; Kang, D. G.; Song, Y. H.; Cha, H. J. The adhesive properties of coacervated recombinant hybrid mussel adhesive proteins. *Biomaterials* **2010**, *31*, 3715−22.
(323) Choi, Y. S.; Kang, D. G.; Lim, S.; Yang, Y. J.; Kim, C. S.; Cha, H. J. Recombinant mussel adhesive protein fp-5 (MAP fp-5) as a bulk bioadhesive and surface coating material. *Biofouling* **2011**, *27*, 729−37.
(324) Aldred, N. Transdisciplinary approaches to the study of adhesion and adhesives in biological systems. *Philos. Trans. R. Soc., B* **2019**, *374*, 20190191.
(325) Morales-Garcia, A. L.; Bailey, R. G.; Jana, S.; Burgess, J. G. The role of polymers in cross-kingdom bioadhesion. *Philos. Trans. R. Soc., B* **2019**, *374*, 20190192.

(326) Guerette, P. A.; Hoon, S.; Seow, Y.; Raida, M.; Masic, A.; Wong, T.; Ho, V. H. B.; Kong, K. W.; Demirel, M. C.; Pena-Francesch, A.; Amini, S.; Tay, G. Z.; Ding, D.; Miserez, A. Accelerating the design of biomimetic materials by integrating RNA-seq with proteomics and materials science. *Nat. Biotechnol.* **2013**, *31*, 908−915.
(327) Bakshani, C. R.; Morales-Garcia, A. L.; Althaus, M.; Wilcox, M. D.; Pearson, J. P.; Bythell, J. C.; Burgess, J. G. Evolutionary conservation of the antimicrobial function of mucus: a first defence against infection. *NPJ. Biofilms and Microbiomes* **2018**, *4*, 14 DOI: 10.1038/s41522-018-0057-2.
(328) Roy, C. K.; Guo, H. L.; Sun, T. L.; Ihsan, A. B.; Kurokawa, T.; Takahata, M.; Nonoyama, T.; Nakajima, T.; Gong, J. P. Self-Adjustable Adhesion of Polyampholyte Hydrogels. *Adv. Mater.* **2015**, *27*, 7344−7348.
(329) Han, W.; et al. Biofilm-inspired adhesive and antibacterial hydrogel with tough tissue integration performance for sealing hemostasis and wound healing. *Bioactive Materials* **2020**, *5*, 768−778.
(330) Almeida, M.; Reis, R. L.; Silva, T. H. Marine invertebrates are a source of bioadhesives with biomimetic interest. *Mater. Sci. Eng., C* **2020**, *108*, 110467.
(331) Lengerer, B.; Algrain, M.; Lefevre, M.; Delroisse, J.; Hennebert, E.; Flammang, P. Interspecies comparison of sea star adhesive proteins. *Philos. Trans. R. Soc., B* **2019**, *374*, 20190195.
(332) Pjeta, R.; Lindner, H.; Kremser, L.; Salvenmoser, W.; Sobral, D.; Ladurner, P.; Santos, R. Integrative Transcriptome and Proteome Analysis of the Tube Foot and Adhesive Secretions of the Sea Urchin Paracentrotus lividus. *Int. J. Mol. Sci.* **2020**, *21*, 946.
(333) Rittigstein, P.; Priestley, R. D.; Broadbelt, L. J.; Torkelson, J. M. Model polymer nanocomposites provide an understanding of confinement effects in real nanocomposites. *Nat. Mater.* **2007**, *6*, 278−282.
(334) Jancar, J.; Douglas, J.; Starr, F. W.; Kumar, S.; Cassagnau, P.; Lesser, A.; Sternstein, S. S.; Buehler, M. Current issues in research on structure−property relationships in polymer nanocomposites. *Polymer* **2010**, *51*, 3321−3343.

https://doi.org/10.1021/acs.macromol.1c01182
Macromolecules 2021, 54, 10617−10644